

# From a Frequency-Domain Willems' Lemma to Data-Driven Predictive Control

Tomas J. Meijer, *Member, IEEE*, Koen J. A. Scheres, *Member, IEEE*, Sven A. N. Nouwens, Victor S. Dolk, and W. P. M. H. (Maurice) Heemels, *Fellow, IEEE*

**Abstract**—Willems' fundamental lemma has recently received an impressive amount of attention from the (data-driven) control community. In this paper, we formulate a version of this celebrated result based on frequency-domain data. In doing so, we bridge the gap between recent developments in data-driven analysis and control, and the readily-available techniques and extensive expertise for non-parametric frequency-domain identification in academia and industry. In addition, we generalize our results to allow multiple frequency-domain data sets to be carefully combined to form a sufficiently rich data set. Building on these results, we propose a data-driven predictive control scheme based on measured frequency-domain data of the plant. This novel scheme provides a frequency-domain counterpart of the well-known data-enabled predictive control scheme DeePC based on time-domain data. We prove that, under appropriate conditions, the new frequency-domain data-driven predictive control (FreePC) scheme is equivalent to the corresponding DeePC scheme, and we demonstrate the benefits of FreePC and the use of frequency-domain data in a numerical case study. These benefits include the ability to collect data in closed loop with a pre-stabilizing controller, dealing with noisy data, without increasing computational complexity, and intuitively visualizing the uncertainty in the frequency-domain data. In addition, we further showcase the potential of our frequency-domain Willems' fundamental lemma in applications to data-driven simulation, and the linear-quadratic regulator (LQR) problem. Finally, we show that our results can be used to evaluate the transfer function of the system at a desired frequency based on a finite amount of frequency-domain data.

**Index Terms**—Data-driven control, frequency-response function measurements, model predictive control, DeePC

## I. INTRODUCTION

**W**ILLEMS' (fundamental) lemma (WFL) states that, for a linear time-invariant (LTI) system, a single data sequence, which consists of  $N$  time-domain input-output data points with a persistently-exciting (PE) input, can be used to characterize all possible input-output solutions of length  $L < N$  of the system [1], [2]. An immediate consequence of WFL, which was originally introduced in [3], is that such a persistently-exciting data sequence describes the entire behavior of the data-generating system [4]. This result does not only enable the system to be identified using subspace identification methods [5], but has also caused WFL to become one of the cornerstones of modern data-driven control. The

desire to extend these remarkable results to more diverse and increasingly more complicated systems has inspired a considerable body of work aimed at generalizing/adapting WFL to accommodate such systems. Some examples include nonlinear systems [1], [6], linear parameter-varying systems [2], descriptor systems [7], [8], stochastic systems [8], [9], and continuous-time systems [10] to name a few. We refer to [8, Table 1] for a more complete overview.

One particularly impactful application of the original time-domain WFL in recent years has been data-enabled predictive control (DeePC), which uses WFL as a data-driven substitute for the prediction model in predictive control [11], see [12] for a recent survey on this lively topic. The success of DeePC has, in turn, inspired many important extensions to accommodate, e.g., descriptor systems [7], linear parameter-varying systems [13], bilinear systems [14], nonlinear systems [15], [16], [17], [18], and stochastic systems [19], [20].

Interestingly, none of the aforementioned works, either on WFL or the derived data-driven predictive control schemes, deals with frequency-domain data. To some extent this is surprising as classical (loop-shaping) control methodologies are often designed based on *non-parametric* frequency-domain models/data [21], [22]. As a consequence, their historic popularity has resulted in an abundance of frequency-domain identification techniques and data, as well as expertise on collecting, interpreting and exploiting such data for control purposes. Unlike the existing formulations, a frequency-domain version of WFL would enable us to not only exploit the available data, but also use the available expertise and (identification) techniques to our benefit *without* the need to turn the frequency-domain data into a parametric (state-space) model. In particular, frequency-domain (identification) techniques offer some significant benefits such as, e.g., dealing with data affected by noise and transient phenomena, see, e.g., [23], [24], as well as the ability to perform closed-loop frequency-response-function (FRF) measurements to deal with unstable systems, see, e.g., [25], [23]. The only frequency-domain version of WFL known to the authors is given in [26]. Unfortunately, this interesting result is only shown to apply to stable systems, and it does not account for conjugate symmetry in the data that arises due to the data-generating system being real. Another relevant work connecting WFL to the frequency domain is [27], in which time-domain data is used to compute the frequency response of the system through WFL. This essentially complements the problem addressed in the present paper of using frequency-domain data to characterize (in time domain) the dynamics of the system. Some note-

This research received funding from the European Research Council (ERC) under the Advanced ERC grant agreement PROACTHIS, no. 101055384.

The authors are with the Control Systems Technology Section, Department of Mechanical Engineering, Eindhoven University of Technology, P.O. Box 513, 5600 MB Eindhoven, The Netherlands (e-mail: {t.j.meijer; k.j.a.scheres; s.a.n.nouwens; v.s.dolk; m.heemels}@tue.nl).

worthy connections between predictive control and frequency domain are found in, e.g., [28], [29], [30], which present frequency-domain *tuning* approaches, and [31] which presents a scheme based on wavelets that are able to extract frequency content from time-domain data. Despite these works, generally speaking, model/data-driven predictive control are purely time-domain control techniques, and direct use of frequency-domain data/models of the plant (without the need to turn it into a parametric (state-space) model) is not yet possible.

To address the gap identified above, this paper presents a version of WFL based on frequency-domain data, which forms the frequency-domain counterpart of the original time-domain WFL. We also take into account the conjugate symmetry of the frequency-domain data, and, thereby, fully exploit the available information (resulting in up to 2 orders of PE per excited frequency). Compared to the preliminary conference version of this work [32], we not only include detailed proofs of the frequency-domain WFL, but we also present an extension that allows the use of multiple data sets, which is particularly relevant when dealing with multi-input multi-output (MIMO) systems. This extension complements a similar extension to multiple data sets presented in [4] for the original time-domain WFL. We also illustrate several important applications of our results, which are new compared to the preliminary version [32], including frequency-domain data-driven simulation, linear quadratic regulator (LQR) design, and a method to evaluate the transfer function of the unknown system at a desired complex frequency based on a finite amount of frequency-domain data. The latter complements a similar result based on time-domain data found in [27]. Finally, we use our results to propose a frequency-domain data-driven predictive control (FreePC) scheme, which provides a frequency-domain counterpart of the celebrated DeePC scheme that is based on the original time-domain version of WFL. In fact, we prove that, under appropriate conditions, the new FreePC scheme is equivalent to the corresponding DeePC scheme. We also showcase some key benefits of FreePC and the use of frequency-domain data in general in a numerical case study. These benefits include the ability to collect data in closed loop with a pre-stabilizing controller so that our results may also be applied to unstable systems, dealing with noisy data, without increasing computational complexity, and intuitively visualizing the uncertainty in the data as a result of noise and transient phenomena.

The remainder of this paper is organized as follows. In Section II, some relevant preliminaries and notation are introduced. Section III formally introduces the considered problem setting. Section IV and Section VI present, respectively, the frequency-domain WFL and a frequency-domain data-driven predictive control scheme, which form our main contributions. In Section V, we investigate several interesting applications of the frequency-domain WFL. Finally, Section VII provides our conclusions and all the proofs of our results can be found in the Appendix.

## II. PRELIMINARIES

### A. Basic notation

Let  $\mathbb{R}$  denote the field of reals,  $\mathbb{C}$  the complex plane, and  $\mathbb{Z}$  the integers. We denote  $\mathbb{Z}_{[n,m]} = \{n, n+1, \dots, m\}$  and  $\mathbb{Z}_{\geq n} = \{n, n+1, \dots\}$ , where  $n, m \in \mathbb{Z}$  and  $n \geq m$ . The imaginary unit is denoted  $j$ , i.e.,  $j^2 = -1$ . For a complex-valued matrix  $A \in \mathbb{C}^{n \times m}$ ,  $A^\top$ ,  $A^H$ ,  $A^*$  and  $A^\dagger$  denote its transpose, its complex-conjugate transpose, its complex conjugate, and its pseudo-inverse, respectively, whereas  $\Re A$  and  $\Im A$  denote its real and imaginary part, and  $A_\perp$  denotes any matrix whose columns form a basis for  $\ker A$ . Let  $(u_1, u_2, \dots, u_q) := \text{col}(u_1, u_2, \dots, u_q)$  for any vectors  $u_i \in \mathbb{K}^{n_i}$ ,  $i \in \{1, 2, \dots, q\}$ . We use  $\otimes$  to denote the Kronecker product, and  $e_i = (0_{i-1}, 1, 0_{n-i}) \in \mathbb{R}^n$ ,  $i \in \mathbb{Z}_{[1,n]}$ , to denote the  $i$ -th  $n$ -dimensional elementary basis vector.

### B. Persistence of excitation

Consider the (time-domain) signal  $v : \mathbb{Z} \rightarrow \mathbb{R}^{n_v}$ . We denote with  $v_{[r,s]}$ ,  $r, s \in \mathbb{Z}$  with  $r \leq s$ , the vectorized restriction of  $v$  to the interval  $\mathbb{Z}_{[r,s]}$ , i.e.,

$$v_{[r,s]} := [v_r^\top \quad v_{r+1}^\top \quad \dots \quad v_s^\top]^\top.$$

With some abuse of notation, we also use the notation  $v_{[r,s]}$  to refer to the real-valued sequence  $\{v_k\}_{k \in \mathbb{Z}_{[r,s]}}$ . We define the Hankel matrix of depth  $L \leq s - r + 1$  generated by  $v_{[r,s]}$  as

$$H_L(v_{[r,s]}) := \begin{bmatrix} v_r & v_{r+1} & \dots & v_{s-L+1} \\ v_{r+1} & v_{r+2} & \dots & v_{s-L+2} \\ \vdots & \vdots & \ddots & \vdots \\ v_{r+L-1} & v_{r+L} & \dots & v_s \end{bmatrix}.$$

Next, we recall the definition of persistence of excitation.

*Definition 1:* The real-valued sequence  $v_{[0,N-1]}$  is said to be persistently exciting (PE) of order  $L \in \mathbb{Z}_{[1,N]}$ , if the matrix  $H_L(v_{[0,N-1]})$  has full row rank.

Note that the scope of Definition 1 is explicitly restricted to real-valued sequences. This will become important when, in the sequel, we also encounter frequency-domain, which is complex-valued.

### C. Willems' fundamental lemma

Consider the LTI system  $\Sigma$  described by

$$\Sigma : \begin{cases} x_{k+1} &= Ax_k + Bu_k, \\ y_k &= Cx_k + Du_k, \end{cases} \quad (1a)$$

$$(1b)$$

where  $x_k \in \mathbb{R}^{n_x}$ ,  $u_k \in \mathbb{R}^{n_u}$  and  $y_k \in \mathbb{R}^{n_y}$  denote, respectively, the state, control input, and measured output (signals) of  $\Sigma$  at time  $k \in \mathbb{Z}$ . Let  $\ell_\Sigma \in \mathbb{Z}_{[1,n_x]}$  denote the observability index of  $\Sigma$ , i.e., the smallest integer for which the observability matrix

$$\mathcal{O}_{\ell_\Sigma} := [C^\top \quad (CA)^\top \quad \dots \quad (CA^{\ell_\Sigma-1})^\top]^\top \quad (2)$$

satisfies  $\text{rank } \mathcal{O}_{\ell_\Sigma} = \text{rank } \mathcal{O}_{n_x}$ . The system  $\Sigma$ , i.e., the matrices  $(A, B, C, D)$ , are unknown. We assume the following regarding  $\Sigma$ .

*Assumption 1:* The pair  $(A, B)$  is controllable.

As mentioned before, WFL can be used to characterize the entire behavior of  $\Sigma$  using a single sequence of input-output data generated by  $\Sigma$ , of which the input sequence is PE. The input-output trajectories introduced below formalize this notion of data sequences.

*Definition 2:* A pair of real-valued length- $N$  sequences  $(u_{[0,N-1]}, y_{[0,N-1]})$  is called an input-output trajectory of  $\Sigma$  in (1), if there exists a state sequence  $x_{[0,N-1]}$  satisfying (1a) for  $k \in \mathbb{Z}_{[0,N-2]}$  and (1b) for  $k \in \mathbb{Z}_{[0,N-1]}$ . In that case, the triplet  $(u_{[0,N-1]}, x_{[0,N-1]}, y_{[0,N-1]})$  is called an input-state-output trajectory of  $\Sigma$ .

Next, we recall WFL, which was originally published in [3].

*Lemma 1:* Let  $(\hat{u}_{[0,N-1]}, \hat{x}_{[0,N-1]}, \hat{y}_{[0,N-1]})$  be an input-state-output trajectory<sup>1</sup> of  $\Sigma$  in (1) satisfying Assumption 1. Suppose that  $\hat{u}_{[0,N-1]}$  is PE of order  $L + n_x$  with  $L \in \mathbb{Z}_{\geq 1}$ . Then, the following statements hold:

(i) The matrix

$$\begin{bmatrix} H_1(x_{[0,N-L]}) \\ H_L(u_{[0,N-1]}) \end{bmatrix}$$

has full row rank;

(ii) The pair of real-valued sequences  $(u_{[0,L-1]}, y_{[0,L-1]})$  of length  $L$  is an input-output trajectory of  $\Sigma$ , if and only if there exists  $g \in \mathbb{R}^{N-L+1}$  such that

$$\begin{bmatrix} u_{[0,L-1]} \\ y_{[0,L-1]} \end{bmatrix} = \begin{bmatrix} H_L(\hat{u}_{[0,L-1]}) \\ H_L(\hat{y}_{[0,L-1]}) \end{bmatrix} g.$$

Lemma 1 is a combination of [3, Corollary 2.(iii)], which is Lemma 1.(i), and [3, Theorem 1], which is Lemma 1.(ii). Lemma 1.(i) means that a powerful rank condition on a particular matrix containing both state and input data can be achieved by exciting  $\Sigma$  with an input of sufficient order of PE, which has proved useful in, e.g., subspace identification [5] and data-driven state-feedback synthesis [33], [4], [34]. Lemma 1.(ii), on the other hand, expresses all possible input-output trajectories of  $\Sigma$  of length  $L$  as a linear combination of time-shifted windows of a single input-output trajectory of length  $N$  collected off-line using an input sequence of sufficiently-high PE order. This result has found numerous applications in system identification, see, e.g., [5], [35], [36], it has also proved remarkably powerful in the context of data-driven *predictive* control over the recent years, see, e.g., [11], [37], [13], [7]. Rather than using a single persistently-exciting input-output trajectory, Lemma 1 has also been extended to allow multiple input-output trajectories that are collectively but not necessarily individually PE [4]. In the next section, we briefly summarize how Lemma 1 is used in data-driven predictive control.

#### D. Data-driven predictive control

In DeePC [11], Lemma 1 is used to obtain a prediction model directly in terms of (time-domain) data. We complete this preliminaries section by briefly recalling the working principles of DeePC. Let  $v_{i,k} \in \mathbb{R}^{n_v}$ ,  $i \in \mathbb{Z}_{[m,n]}$  with  $m, n \in \mathbb{Z}$  and  $n \geq m$ , denote the prediction of  $v_{k+i}$  made at time  $k \in \mathbb{Z}$ .

<sup>1</sup>We use the accent  $\hat{\cdot}$  to denote data that was collected previously/off-line. For example,  $\hat{y}_{[0,M-1]}$  denotes the sequence of outputs collected off-line.

We introduce the notation  $v_{[m,n],k} = \{v_{i,k}\}_{i \in \mathbb{Z}_{[m,n]}}$  to refer to the sequence of such predictions made at time  $k \in \mathbb{Z}$  or to refer to the vectorized predicted sequence, i.e.,

$$v_{[m,n],k} = [v_{m,k}^\top \quad v_{m+1,k}^\top \quad \cdots \quad v_{n,k}^\top]^\top.$$

Since DeePC is not based on a particular realization of  $\Sigma$ , its state is fundamentally unknown. To ensure that the initial state of the prediction model is consistent with the internal state of  $\Sigma$ , an initial input-output trajectory  $(u_{[k-\bar{T},k-1]}, y_{[k-\bar{T},k-1]})$ ,  $\bar{T} \in \mathbb{Z}_{\geq 1}$ , is prepended. Note that, since we do not assume observability of  $\Sigma$ , this internal state is not necessarily uniquely determined by the initial input-output trajectory. However, by using an initial trajectory of length  $\bar{T} \in \mathbb{Z}_{\geq \ell_\Sigma}$ , the observable part of the state is uniquely determined and, as a result, the future output is, for any given input sequence, also unique.

Let  $T \in \mathbb{Z}_{\geq 1}$  be the prediction horizon and let  $(\hat{u}_{[0,N-1]}, \hat{y}_{[0,N-1]})$  be an input-output trajectory of  $\Sigma$ , with  $\hat{u}_{[0,N-1]}$  being PE of order  $\bar{T} + T + n_x \geq \ell_\Sigma + T + n_x$ . Then, at every  $k \in \mathbb{Z}_{\geq 0}$ , given the initial input-output trajectory  $(u_{[k-\bar{T},k-1]}, y_{[k-\bar{T},k-1]})$ , DeePC [11] solves the finite-horizon optimal control problem

$$\begin{aligned} \min_{\substack{\hat{u}_{[0,T-1],k}, \\ y_{[0,T-1],k}, \\ g_k, \sigma_k}} \quad & \lambda_\sigma \|\sigma_k\|_1 + \lambda_g \|g_k\|_1 + \sum_{i \in \mathbb{Z}_{[0,T-1]}} \ell(y_{i,k}, u_{i,k}), \\ \text{s. t.} \quad & \begin{bmatrix} u_{[k-\bar{T},k-1]} \\ \text{---} \\ u_{[0,T-1],k} \\ y_{[k-\bar{T},k-1]} + \sigma_k \\ y_{[0,T-1],k} \end{bmatrix} = \begin{bmatrix} H_{\bar{T}+T}(\hat{u}_{[0,N-1]}) \\ \text{---} \\ H_{\bar{T}+T}(\hat{y}_{[0,N-1]}) \end{bmatrix} g_k, \quad (3) \\ & u_{i,k} \in \mathbb{U}, \quad y_{i,k} \in \mathbb{Y}, \quad \text{for all } i \in \mathbb{Z}_{[0,T-1]}, \end{aligned}$$

where  $\mathbb{U}$  and  $\mathbb{Y}$  denote the set of admissible inputs and outputs, respectively, while  $\ell: \mathbb{R}^{n_y} \times \mathbb{R}^{n_u} \rightarrow \mathbb{R}_{\geq 0}$  denotes the stage cost. The decision variables in (3) are  $g_k \in \mathbb{R}^{N-T-\bar{T}+1}$ ,  $\sigma_k \in \mathbb{R}^{\bar{T}n_y}$ , and the predicted inputs and outputs  $u_{i,k}$  and  $y_{i,k}$ ,  $i \in \mathbb{Z}_{[0,T-1]}$ , respectively. Here,  $\sigma_k$  is an auxiliary slack variable and  $\lambda_\sigma, \lambda_g \in \mathbb{R}_{>0}$  are regularization parameters [11]. These regularization parameters and slack variables are needed to deal with noise in the off-line data as well as the initial output trajectory  $y_{[k-\bar{T},k-1]}$ . In the noiseless/nominal case, however, we can use  $\lambda_g = 0$  and  $\sigma_k = 0$ . To turn (3) into a feedback policy, denote by  $u_{[0,T-1],k}^* = \{u_{i,k}^*\}_{i \in \mathbb{Z}_{[0,T-1]}}$  the optimal control action computed at time  $k$  by solving (3). DeePC implements the first element of  $u_{[0,T-1],k}^*$ , i.e.,  $u_k = u_{0,k}^*$ , and solves (3) at time  $k+1$  using the updated initial input-output trajectory  $(u_{[k-\bar{T}+1,k]}, y_{[k-\bar{T}+1,k]})$ , thereby creating a (receding-horizon) feedback policy.

### III. PROBLEM SETTING

Throughout this paper, we consider the LTI system  $\Sigma$  introduced in (1) satisfying Assumption 1. We assume that  $\Sigma$  itself, so  $(A, B, C, D)$  in (1), is unknown, and that, instead, we are given (sampled) frequency-domain data. To formalize this notion of frequency-domain data, we first recall that the spectrum  $V: \mathbb{W} \rightarrow \mathbb{C}^{n_v}$ , with  $\mathbb{W} := (-\pi, \pi]$ , of the time-domain sequence  $\{v_k\}_{k \in \mathbb{Z}}$ , with  $v_k \in \mathbb{R}^{n_v}$  for all  $k \in \mathbb{Z}$ ,

is obtained by taking the discrete-time Fourier transform (DTFT), i.e.,

$$V(\omega) = \sum_{k \in \mathbb{Z}} v_k e^{-j\omega k}.$$

We also recall that, since  $\{v_k\}_{k \in \mathbb{Z}}$  is real-valued, the spectrum  $V$  is symmetric, i.e.,  $V(\omega) = V^*(-\omega)$  for all  $\omega \in \mathbb{W}$ .

Consider an equidistant frequency grid<sup>2</sup> consisting of the  $M \in \mathbb{Z}_{\geq 1}$  frequencies

$$\hat{\omega}_k = \frac{\pi k}{M}, \quad k \in \mathbb{Z}_{[0, M-1]}. \quad (4)$$

We denote the sequence of these frequencies as  $\hat{\omega}_{[0, M-1]} := \{\hat{\omega}_k\}_{k \in \mathbb{Z}_{[0, M-1]}}$ , which satisfies  $\hat{\omega}_{[0, M-1]} \subset \mathbb{W}$ . Such a grid of (normalized) frequencies is commonly used in, e.g., frequency-domain identification literature [23]. We consider frequency-domain data that consists of sequences  $\hat{V}_{[0, M-1]} = \{\hat{V}_k\}_{k \in \mathbb{Z}_{[0, M-1]}}$ , with  $\hat{V}_k = \hat{V}(\hat{\omega}_k)$  for all  $k \in \mathbb{Z}_{[0, M-1]}$ , of samples of such spectra at the frequencies in  $\hat{\omega}_{[0, M-1]}$ . Since we can exploit the symmetry of  $\hat{V}$ , we only store frequencies in  $[0, \pi)$  in  $\hat{\omega}_{[0, M-1]}$ . In the remainder of this paper, we use lower case, e.g.,  $v_{[0, N-1]}$ , to refer to real-valued time-domain sequences, while the upper case, e.g.,  $V_{[0, M-1]}$  is used to refer to complex-valued frequency-domain sequences.

In particular, our frequency-domain data consists, depending on the precise application, of pairs of sequences  $(\hat{U}_{[0, M-1]}, \hat{Y}_{[0, M-1]})$  or  $(\hat{U}_{[0, M-1]}, \hat{X}_{[0, M-1]})$  containing samples of the input and, respectively, the corresponding output or state spectrum of  $\Sigma$ . To formalize this, we recall that the transfer function  $H : \mathbb{C} \rightarrow \mathbb{C}^{n_v \times n_u}$  of  $\Sigma$  is given by

$$H(z) = C(zI - A)^{-1}B + D, \quad z \in \mathbb{C}.$$

*Definition 3:* A pair of complex-valued length- $M$  sequences  $(\hat{U}_{[0, M-1]}, \hat{Y}_{[0, M-1]})$  is called an input-output spectrum of  $\Sigma$ , if there exists a state spectrum  $\hat{X}_{[0, M-1]}$  satisfying

$$e^{j\hat{\omega}_k} \hat{X}_k = A\hat{X}_k + B\hat{U}_k, \quad (5a)$$

$$\hat{Y}_k = C\hat{X}_k + D\hat{U}_k \quad (5b)$$

for all  $k \in \mathbb{Z}_{[0, M-1]}$ . In that case, the triplet  $(\hat{U}_{[0, M-1]}, \hat{X}_{[0, M-1]}, \hat{Y}_{[0, M-1]})$  is called an input-state-output spectrum of  $\Sigma$ , and the pair  $(\hat{U}_{[0, M-1]}, \hat{X}_{[0, M-1]})$  is called an input-state spectrum of  $\Sigma$ .

Interestingly, Definition 3 includes the important case, where we are given FRF measurements  $\{H(e^{j\hat{\omega}_k})\}_{k \in \mathbb{Z}_{[0, M-1]}}$  to be used as our frequency-domain data, as detailed in Example 1 below. Note that Definition 3 implicitly restricts the frequency-domain data to be obtained from steady-state, i.e., periodic, time-domain data due to the absence of transient phenomena in (5). Definition 3 is also commonly used in subspace identification literature, see, e.g., [38], [39], [40]. A practical and simple method to obtain data that adheres to Definition 3 is, as illustrated in Example 3, by measuring sufficiently long for the transient to dampen out and, subsequently, discarding the initial part of the data where transient phenomena play a significant role. We also note that  $\hat{X}_k$  can

<sup>2</sup>This choice is made for notational convenience and our results readily extend to non-equidistant frequency grids (see also Remark 1).

be eliminated from (5) such that  $(\hat{U}_{[0, M-1]}, \hat{Y}_{[0, M-1]})$  is an input-output spectrum of  $\Sigma$ , if and only if

$$\hat{Y}_k = H(e^{j\hat{\omega}_k})\hat{U}_k,$$

for all  $k \in \mathbb{Z}_{[0, M-1]}$ .

*Example 1 (Incorporating FRF measurements):* Suppose that  $\Sigma$  is a single-input single-output (SISO) system and that we are given FRF measurements  $\{H(e^{j\hat{\omega}_k})\}_{k \in \mathbb{Z}_{[0, M-1]}}$ , of a system  $\Sigma$ . We can incorporate this frequency-domain data by setting  $\hat{Y}_k = H(e^{j\hat{\omega}_k})\hat{U}_k$  and  $\hat{U}_k = 1$  for all  $k \in \mathbb{Z}_{[0, M-1]}$ . The input-output spectrum  $\{\hat{U}_{[0, M-1]}, \hat{Y}_{[0, M-1]}\}$  then comprises our frequency-domain data. If  $\Sigma$  is a MIMO system, however, we can, even if we are given FRF measurements  $\{H(e^{j\hat{\omega}_k})\}_{k \in \mathbb{Z}_{[0, M-1]}}$  containing all input directions at each frequency, only incorporate a single input direction  $r_k \in \mathbb{C}^{n_u}$  for each  $k \in \mathbb{Z}_{[0, M-1]}$  this way, i.e., by setting  $\hat{Y}_k = H(e^{j\hat{\omega}_k})r_k$  and  $\hat{U}_k = r_k$  for all  $k \in \mathbb{Z}_{[0, M-1]}$ . To deal with this, we present a natural extension of our results (see Theorem 2 below), where our data consists of a collection of multiple input-output spectra, which enables us to utilize all available data effectively also in the MIMO case.

*Remark 1:* The results in the sequel also readily apply if the frequencies  $\hat{\omega}_{[0, M-1]}$  lie on a non-equidistant grid which does not necessarily contain  $\hat{\omega}_0 = 0$ , as shown in [41]. In fact, to adhere to the conditions in Definition 3, [41] requires the frequency-domain data to be obtained from *periodic* time-domain data, which implies the existence of the greatest common divisor of the excited frequencies. Hence, we can always define a grid as in (4) (possibly containing many unexcited frequencies, for which  $\hat{U}_k = 0$ ,  $\hat{X}_k = 0$ , and  $\hat{Y}_k = 0$ ) by choosing  $M$  to be sufficiently large.

As indicated in the introduction, almost all existing variants of WFL use time-domain data and much less effort has been directed towards data-driven control based on WFL using frequency-domain data. In this paper, our goal is to fill the resulting gaps in the literature by formulating a version of WFL based on frequency-domain data and, subsequently, using it for data-driven (predictive) control.

## IV. WILLEMS' LEMMA IN FREQUENCY DOMAIN

In this section, we subsequently introduce the notion of persistence of excitation for frequency-domain data and use such data to formulate a frequency-domain version of Willems' fundamental lemma. Analogous to [4], we also present extensions of these results to exploit multiple frequency-domain data sets.

### A. Persistence of excitation in frequency domain

The original WFL requires the considered time-domain data to be sufficiently "rich", which is formalized in the notion of persistence of excitation (see Definition 1). It should come as no surprise that we require also the frequency-domain data to be sufficiently "rich", which we will now formalize by defining PE for the complex-valued sequence  $V_{[0, M-1]}$  introduced in the previous section. To this end, let, for  $L \in \mathbb{Z}_{\geq 1}$ ,  $F_L : \mathbb{C}^{n_v(m-n+1)} \rightarrow \mathbb{C}^{n_v L \times (m-n+1)}$ , where  $m, n \in \mathbb{Z}_{\geq 0}$  with

$n \geq m$ , be the matrix-valued function of a sequence of length  $m - n + 1$  given by

$$F_L(V_{[m,n]}) = [W_L(e^{j\hat{\omega}_m}) \otimes V_m \quad \dots \quad W_L(e^{j\hat{\omega}_n}) \otimes V_n], \quad (6)$$

where  $W_L(z) := [1 \quad z \quad \dots \quad z^{L-1}]^\top$ ,  $z \in \mathbb{C}$ .

Using  $F_L$  and the symmetry of the underlying spectrum, we define PE for the complex-valued sequence  $V_{[0,M-1]}$  below.

**Definition 4:** The complex-valued sequence  $V_{[0,M-1]} \in \mathbb{C}^{n_v M}$  of length  $M$  is said to be persistently exciting of order  $L \in \mathbb{Z}_{[1,2M-1]}$ , if the matrix

$$[F_L(V_{[0,M-1]}) \quad F_L^*(V_{[1,M-1]})]$$

has full row rank.

The following remarks are in order regarding Definition 4. First, observe that Definition 4 exploits the symmetry in the underlying spectrum by including also the complex conjugate  $F_L^*(V_{[1,M-1]})$  in the rank condition. This term corresponds to the spectral content at the negative frequencies. Note that, since the complex-conjugate data at  $\hat{\omega}_0 = 0$  does not add any additional information, we only include the complex-conjugate data for  $V_{[1,M-1]}$  (i.e., starting from  $V_1$  instead of  $V_0$ ). Let

$$T_{\mathbb{R}} := \frac{1}{2} \begin{bmatrix} 2 & 0 & 0 \\ 0 & I_{M-1} & -jI_{M-1} \\ 0 & I_{M-1} & jI_{M-1} \end{bmatrix}.$$

By exploiting the conjugate symmetry, we find that the rank condition in Definition 4 is equivalent to the real-valued matrix

$$\begin{bmatrix} F_L(V_{[0,M-1]}) & F_L^*(V_{[1,M-1]}) \end{bmatrix} T_{\mathbb{R}} = \begin{bmatrix} \Re F_L(V_{[0,M-1]}) & \Im F_L(V_{[1,M-1]}) \end{bmatrix}$$

having full row rank. Secondly, the rank condition in Definition 4 implies that  $2M - 1 \geq Ln_v$ . Data at any non-zero frequency, i.e., any frequency in  $\hat{\omega}_{[1,M-1]}$ , yields at most 2 orders of PE because the complex conjugate also contributes, whereas the data at  $\hat{\omega}_0 = 0$  contributes at most 1 order of PE.

In Section IV-C, we extend Definition 4 to allow the combination of multiple frequency-domain data sets that are not PE when considered individually but nonetheless are collectively sufficiently ‘‘rich’’.

### B. A frequency-domain Willems’ fundamental lemma

Next, we introduce our frequency-domain version of WFL [3], which provides counterparts to both statements in Lemma 1 based on frequency-domain data.

**Theorem 1:** Let  $(\hat{U}_{[0,M-1]}, \hat{X}_{[0,M-1]}, \hat{Y}_{[0,M-1]})$  be an input-state-output spectrum of  $\Sigma$  in (1) satisfying Assumption 1. Suppose that  $\hat{U}_{[0,M-1]}$  is PE of order  $L + n_x$ . Then, the following statements hold:

(i) The matrix

$$\begin{bmatrix} F_1(\hat{X}_{[0,M-1]}) & F_1^*(\hat{X}_{[1,M-1]}) \\ F_L(\hat{U}_{[0,M-1]}) & F_L^*(\hat{U}_{[1,M-1]}) \end{bmatrix}$$

has full row rank;

(ii) The pair of real-valued (time-domain) sequences  $(u_{[0,L-1]}, y_{[0,L-1]})$  of length  $L$  is an input-output trajectory of  $\Sigma$ , if and only if there exist  $G_0 \in \mathbb{R}$  and  $G_1 \in \mathbb{C}^{M-1}$  such that

$$\begin{bmatrix} u_{[0,L-1]} \\ y_{[0,L-1]} \end{bmatrix} = \begin{bmatrix} F_L(\hat{U}_{[0,M-1]}) & F_L^*(\hat{U}_{[1,M-1]}) \\ F_L(\hat{Y}_{[0,M-1]}) & F_L^*(\hat{Y}_{[1,M-1]}) \end{bmatrix} \begin{bmatrix} G_0 \\ G_1 \\ G_1^* \end{bmatrix}.$$

The proof of Theorem 1 can be found in the Appendix. Theorem 1.(i) states that one can render a specific matrix, which contains samples of the state and input spectrum, full row rank by injecting an input spectrum whose order of PE is at least equal to  $n_x + n_u L$ . This result, which provides a frequency-domain counterpart of Lemma 1.(i), is used in proving Theorem 1.(ii). Moreover, its time-domain version has found numerous applications in, for instance, subspace identification, see, e.g., [5], and state-feedback synthesis, see, e.g., [33], [4], [34]. In these applications, Theorem 1.(i) can be used to perform these tasks directly based on frequency-domain data. In fact, in Section V-C, we showcase such an application to obtain an LQR directly in terms of the frequency-domain data. Theorem 1.(ii), on the other hand, provides a counterpart to Lemma 1.(ii) based on frequency-domain data, and states that we can characterize all input-output trajectories of  $\Sigma$  of length  $L$  using samples of its input-output spectrum collected off-line. Importantly, Theorem 1.(ii) can be applied *without* measuring the state spectrum  $\hat{X}_{[0,M-1]}$  as it only uses of the input-output spectrum.

Some further remarks regarding Theorem 1 are in order.

- We see that, analogous to the shift theorem of the DTFT [42], the time delays that are present in the Hankel matrices in Lemma 1 translate to linear phase terms, i.e., the increasing powers of  $e^{j\hat{\omega}_k}$  in  $W_L(e^{j\hat{\omega}_k})$  in Theorem 1;
- Using conjugate symmetry, Theorem 1.(i) is equivalent to the real-valued matrix

$$\begin{bmatrix} F_1(\hat{X}_{[0,M-1]}) & F_1^*(\hat{X}_{[1,M-1]}) \\ F_L(\hat{U}_{[0,M-1]}) & F_L^*(\hat{U}_{[1,M-1]}) \end{bmatrix} T_{\mathbb{R}} = \begin{bmatrix} \Re F_1(\hat{X}_{[0,M-1]}) & \Im F_1(\hat{X}_{[1,M-1]}) \\ \Re F_L(\hat{U}_{[0,M-1]}) & \Im F_L(\hat{U}_{[1,M-1]}) \end{bmatrix}$$

having full row rank. Similarly, we obtain from Theorem 1.(ii) that the pair of real-valued length- $L$  sequences  $(u_{[0,L-1]}, y_{[0,L-1]})$  is an input-output trajectory of  $\Sigma$ , if and only if there exists  $g \in \mathbb{R}^{2M-1}$  such that

$$\begin{bmatrix} u_{[0,L-1]} \\ y_{[0,L-1]} \end{bmatrix} = \begin{bmatrix} \Re F_L(\hat{U}_{[0,M-1]}) & \Im F_L(\hat{U}_{[1,M-1]}) \\ \Re F_L(\hat{Y}_{[0,M-1]}) & \Im F_L(\hat{Y}_{[1,M-1]}) \end{bmatrix} g,$$

where we performed the change of variables

$$g = T_{\mathbb{R}}^{-1} G = \begin{bmatrix} G_0 \\ 2\Re(G_1) \\ -2\Im(G_1) \end{bmatrix}.$$

### C. Extension to multiple data sets

In this section, we provide generalizations of Definition 4 and Theorem 1, which are our frequency-domain notions of

PE and WFL, respectively, to allow for multiple data sets. A similar extension has been proposed for the time-domain WFL in [4] to deal with, e.g., missing data samples and unstable systems. For frequency-domain data, using multiple data sets is natural, if not necessary, because it enables us to incorporate information regarding multiple input directions at the same frequency. As discussed in Example 1, this allows us to use complete FRF measurements of MIMO transfer functions for our data, i.e.,  $\{H(e^{j\hat{\omega}_k})\}_{k \in \mathbb{Z}_{[0, M-1]}}$ , while Theorem 1 can only use the information in  $H(e^{j\hat{\omega}_k})$  for one input direction per frequency. Naturally, we can also use the input-output spectra used to estimate  $H(e^{j\hat{\omega}_k})$  in our data directly.

To enable the use of data containing multiple input directions at the same frequency, we will now introduce the notion of collective persistence of excitation (CPE) [4] for frequency-domain data. In particular, we consider collections of  $E \in \mathbb{Z}_{\geq 1}$  sequences  $\{V_{[0, M-1]}^e\}_{e \in \mathcal{E}}$  with  $V_{[0, M-1]}^e = \{V_k^e\}_{k \in \mathbb{Z}_{[0, M-1]}}$  and  $V_k^e = V^e(\hat{\omega}_k)$  for all  $k \in \mathbb{Z}_{[0, M-1]}$  and  $e \in \mathcal{E} := \mathbb{Z}_{[1, E]}$ . For notational simplicity, we assume that each of the sequences corresponds to the same sequence of frequencies  $\hat{\omega}_{[0, M-1]}$ , which was defined in Section III. If all excited frequencies admit a greatest common divisor, this is without loss of generality because we can always define a common frequency grid and set  $V_k^e = 0$  for the unexcited frequencies per experiment (see also Remark 1). Let, for  $L \in \mathbb{Z}_{\geq 1}$ ,  $\mathcal{F}_L : \mathbb{C}^{n_v(m-n+1)E} \rightarrow \mathbb{C}^{n_v L \times (m-n+1)E}$ , where  $m, n \in \mathbb{Z}_{\geq 0}$  with  $n \geq m$ , be the matrix-valued function of  $E$  sequences of length  $m - n + 1$  given by

$$\mathcal{F}_L(\{V_{[m, n]}^e\}_{e \in \mathcal{E}}) = [W_L(e^{j\hat{\omega}_m}) \otimes [v_m^1 \dots v_m^E] \quad \dots \quad W_L(e^{j\hat{\omega}_n}) \otimes [v_n^1 \dots v_n^E]],$$

which is essentially  $F_L(V_{[m, n]})$  but for multiple data sets that are sorted into one block per frequency.

*Definition 5:* The collection of complex-valued sequences  $\{V_{[0, M-1]}^e\}_{e \in \mathcal{E}}$  of length  $M$  is said to be collectively persistently exciting (CPE) of order  $L \in \mathbb{Z}_{[1, E(2M-1)]}$ , if the matrix

$$[\mathcal{F}_L(\{V_{[0, M-1]}^e\}_{e \in \mathcal{E}}) \quad \mathcal{F}_L^*(\{V_{[1, M-1]}^e\}_{e \in \mathcal{E}})]$$

has full row rank.

*Theorem 2:* Let  $\{(\hat{U}_{[0, M-1]}^e, \hat{X}_{[0, M-1]}^e, \hat{Y}_{[0, M-1]}^e)\}_{e \in \mathcal{E}}$  be a collection of input-state-output spectra of  $\Sigma$  in (1) satisfying Assumption 1. Suppose that  $\{\hat{U}_{[0, M-1]}^e\}_{e \in \mathcal{E}}$  is CPE of order  $L + n_x$ . Then, the following statements hold:

(i) The matrix

$$\begin{bmatrix} \mathcal{F}_1(\{\hat{X}_{[0, M-1]}^e\}_{e \in \mathcal{E}}) & \mathcal{F}_1^*(\{\hat{X}_{[1, M-1]}^e\}_{e \in \mathcal{E}}) \\ \mathcal{F}_L(\{\hat{U}_{[0, M-1]}^e\}_{e \in \mathcal{E}}) & \mathcal{F}_L^*(\{\hat{U}_{[1, M-1]}^e\}_{e \in \mathcal{E}}) \end{bmatrix}$$

has full row rank;

(ii) The pair of real-valued time-domain sequences  $(u_{[0, L-1]}, y_{[0, L-1]})$  of length  $L$  is an input-output

trajectory of  $\Sigma$ , if and only if there exist  $G_0 \in \mathbb{R}^E$  and  $G_1 \in \mathbb{C}^{E(M-1)}$  such that  $G = (G_0, G_1, G_1^*)$  satisfies

$$\begin{bmatrix} u_{[0, L-1]} \\ y_{[0, L-1]} \end{bmatrix} = \begin{bmatrix} \mathcal{F}_L(\{\hat{U}_{[0, M-1]}^e\}_{e \in \mathcal{E}}) & \mathcal{F}_L^*(\{\hat{U}_{[1, M-1]}^e\}_{e \in \mathcal{E}}) \\ \mathcal{F}_L(\{\hat{Y}_{[0, M-1]}^e\}_{e \in \mathcal{E}}) & \mathcal{F}_L^*(\{\hat{Y}_{[1, M-1]}^e\}_{e \in \mathcal{E}}) \end{bmatrix} G.$$

A sketch of proof, which details how the proof of Theorem 1 can be adapted to prove Theorem 2, can be found in the Appendix. Analogous to [4, Theorem 2], which provides an extension of Lemma 1 that allows for the use of multiple (time-domain) data sets, Theorem 2 extends Theorem 1 to carefully combine multiple frequency-domain data sets. In fact, in the case  $E = 1$ , Theorem 2 reduces to Theorem 1. The comments made in Section IV regarding Theorem 1 also apply to Theorem 2.

## V. APPLICATIONS

In this section, we present several interesting applications of Theorem 1, and, in the case of multiple data sets, Theorem 2.

### A. FRF-based simulation

It is well-known that the *steady-state* response of an asymptotically stable system (1) can be simulated using FRF measurements. In this section, we exploit our frequency-domain version of WFL to simulate not only the steady-state behavior of  $\Sigma$  but also its *transient response*, which is, to the best of the authors' knowledge, not possible using existing techniques. Moreover,  $\Sigma$  is also not required to be asymptotically stable here, although the off-line data may have to be collected in closed-loop with a pre-stabilizing controller, as we will illustrate in Example 3. As discussed in Section IV-C, it is natural to consider multiple data sets (i.e., multiple input directions at the same frequency) when dealing with (MIMO) FRF measurements and, as such, we use Theorem 2 as the basis for our FRF-based simulation algorithm.

*Proposition 1:* Let  $\{(\hat{U}_{[0, M-1]}^e, \hat{Y}_{[0, M-1]}^e)\}_{e \in \mathcal{E}}$  be a collection of input-output spectra of  $\Sigma$  in (1) satisfying Assumption 1. Let  $L, L_0 \in \mathbb{Z}_{\geq 1}$  and suppose that  $\{\hat{U}_{[0, M-1]}^e\}_{e \in \mathcal{E}}$  is CPE of order  $L + L_0 + n_x$ . For any length- $L_0$  past input-output trajectory  $(u_{[-L_0, -1]}, y_{[-L_0, -1]})$  of  $\Sigma$  and a (future) input sequence  $u_{[0, L-1]}$ , there exist  $G_0 \in \mathbb{R}^E$  and  $G_1 \in \mathbb{C}^{E(M-1)}$  such that  $G = (G_0, G_1, G_1^*)$  satisfies

$$\begin{bmatrix} u_{[-L_0, L-1]} \\ y_{[-L_0, -1]} \end{bmatrix} = \begin{bmatrix} \mathcal{F}_{L_0+L}(\{\hat{U}_{[0, M-1]}^e\}_{e \in \mathcal{E}}) & \mathcal{F}_{L_0+L}^*(\{\hat{U}_{[1, M-1]}^e\}_{e \in \mathcal{E}}) \\ \mathcal{F}_{L_0}(\{\hat{Y}_{[0, M-1]}^e\}_{e \in \mathcal{E}}) & \mathcal{F}_{L_0}^*(\{\hat{Y}_{[1, M-1]}^e\}_{e \in \mathcal{E}}) \end{bmatrix} G, \quad (7)$$

and  $(u_{[-L_0, L-1]}, y_{[-L_0, L-1]})$  with

$$y_{[-L_0, L-1]} = \begin{bmatrix} \mathcal{F}_{L_0+L}(\{\hat{Y}_{[0, M-1]}^e\}_{e \in \mathcal{E}}) & \mathcal{F}_{L_0+L}^*(\{\hat{Y}_{[1, M-1]}^e\}_{e \in \mathcal{E}}) \end{bmatrix} G \quad (8)$$

is an input-output trajectory of  $\Sigma$ . If, in addition,  $L_0 \geq \ell_\Sigma$ , then  $y_{[0, L-1]}$  is unique.

Proposition 1 can be used to perform data-driven simulation of the unknown system  $\Sigma$  directly based on frequency-domain data of the system. To do so, we determine  $G$  satisfying (7) for the past input-output trajectory  $(u_{[-L_0, -1]}, y_{[-L_0, -1]})$  and the future input sequence  $u_{[0, L-1]}$ , which always exists due to the PE condition. Subsequently, we use the obtained  $G$  to compute the future output sequence  $y_{[0, L-1]}$  from (8). Note that, since we do not assume observability of  $\Sigma$ , the internal state of the system is not necessarily uniquely determined by the initial input-output trajectory. However, the past input-output trajectory ensures that the simulation commences from an initial condition in the set of initial conditions that are consistent with the past input-output trajectory. By using an initial trajectory of length  $L_0 \geq \ell_\Sigma$ , the observable part of the internal state is uniquely determined and, as a result, the future output sequence is, for any given input sequence, also unique. We can also perform a similar change of variables to the one described in Section IV-B to transform the complex-valued equations in Proposition 1 to an equivalent real-valued formulation. In the next two sections, we further investigate the use of Proposition 1 to perform data-driven simulations in some numerical case studies.

*Example 2 (FRF-based simulation using noise-free data):* We consider the unstable batch reactor [43], [4], which we discretize using a sampling time of  $T_s = 0.5\text{s}$  to obtain a system of the form (1) with

$$A = \begin{bmatrix} 2.622 & 0.320 & 1.834 & -1.066 \\ -0.238 & 0.187 & -0.136 & 0.202 \\ 0.161 & 0.789 & 0.286 & 0.606 \\ -0.104 & 0.764 & 0.089 & 0.736 \end{bmatrix}, \quad (9)$$

$$B = \begin{bmatrix} 0.465 & -1.550 \\ 1.314 & 0.085 \\ 2.055 & -0.673 \\ 2.023 & -0.160 \end{bmatrix}, C = \begin{bmatrix} 1 & 0 & 1 & -1 \\ 0 & 1 & 0 & 0 \end{bmatrix} \text{ and } D = 0.$$

To generate the off-line data, we perform  $E = 2$  experiments in which we excite the  $M = 10$  frequencies  $\hat{\omega}_{[0, M-1]}$  in (4). Since we are dealing with noise-free data, we can, for the purposes of this example, generate the off-line data consisting of input-output spectra  $\{(\hat{U}_{[0, M-1]}^e, \hat{Y}_{[0, M-1]}^e)\}_{e \in \mathcal{E}}$  by setting  $\hat{U}_k^e = e_i$  and computing  $\hat{Y}_k^e = H(e^{j\hat{\omega}_k})\hat{U}_k^e$  for all  $k \in \mathbb{Z}_{[0, M-1]}$  and  $e \in \mathcal{E}$ . In practice, we would obviously not be able to generate the data in this way because it requires a priori knowledge of the transfer functions of  $\Sigma$ , however, as we will detail in the next section, closed-loop FRF measurements with a pre-stabilizing controller can be used to collect the required data  $\{(\hat{U}_{[0, M-1]}^e, \hat{Y}_{[0, M-1]}^e)\}_{e \in \mathcal{E}}$ .

The observability index of  $\Sigma$  with (1) is given by  $\ell_\Sigma = 2$ . To perform the simulation, we first generate an initial trajectory of length  $L_0 = \ell_\Sigma$  starting from  $x_{-L_0} = 0$  using a randomly generated input sequence  $u_{[-L_0, -1]}$ . Afterward, we perform a simulation of length  $L = 4$  using Proposition 1 with a randomly generated input sequence  $u_{[0, L-1]}$ . The results are depicted in Fig. 1 along with the true output response of the system  $y_{[-L_0, L-1]}^{\text{true}}$ . We see that, despite the system being unstable, which causes the outputs to grow exponentially, the obtained results closely resemble the true solution, i.e.,

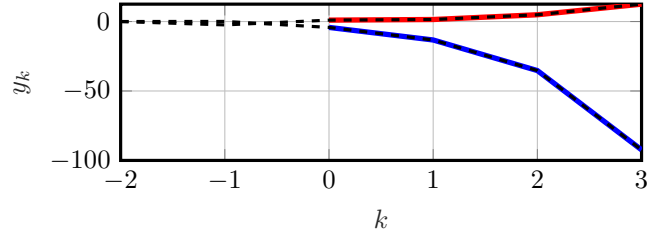


Fig. 1. Data-driven simulation of an unstable batch reactor using noise-free data. We see that the simulated outputs  $y_1$  (—) and  $y_2$  (—) closely resemble the true response (---).

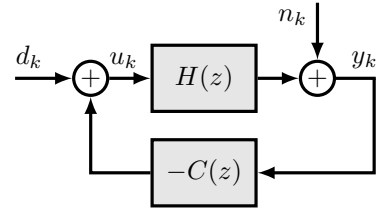


Fig. 2. Closed-loop measurement setup.

$$\|y_{[0, L-1]} - y_{[0, L-1]}^{\text{true}}\|_2 = 6.9857 \cdot 10^{-12} \quad \text{and} \quad \|y_{[0, L-1]} - y_{[0, L-1]}^{\text{true}}\|_2 / \|y_{[0, L-1]}^{\text{true}}\|_2 = 6.9315 \cdot 10^{-14}.$$

*Example 3 (FRF-based simulation using noisy data):* We consider again the unstable batch reactor represented by (1) with (9). However, we now consider a more realistic setting with noisy data. To generate this data, we replace (1b) by

$$y_k = Cx_k + Du_k + n_k,$$

to incorporate measurements noise. Since the system is unstable, we collect our off-line data in a closed-loop measurement setup [25, Chapter 10], as depicted in Fig. 2, with the stabilizing controller

$$C(z) = \frac{1}{1.84(z-1)} \begin{bmatrix} 0 & -5z+1 \\ 2z-1 & 0 \end{bmatrix}.$$

In this closed-loop measurement setup, the input  $u_k \in \mathbb{R}^2$  consists of the output of the controller on top of which we inject a signal  $\{d_k\}_{k \in \mathbb{Z}}$  with  $d_k \in \mathbb{R}^2$  for all  $k \in \mathbb{Z}$ . We conduct two experiments to collect our off-line data, in which we each excite only one element of the injected signal  $d_k$  using a multi-sine. To be precise, for experiment  $e \in \mathcal{E}$ , we inject the signal  $d_k^e$  given by

$$d_k^e = \begin{cases} (10 \sum_{m \in \mathbb{Z}_{[0, M-1]}} \cos(\hat{\omega}_m k + \hat{\phi}_m^e), 0), & \text{if } e = 1, \\ (0, 10 \sum_{m \in \mathbb{Z}_{[0, M-1]}} \cos(\hat{\omega}_m k + \hat{\phi}_m^e)), & \text{if } e = 2, \end{cases}$$

with the  $M = 10$  frequencies  $\hat{\omega}_{[0, M-1]}$  in (4) and random phase shifts  $\{\hat{\phi}_k^e\}_{k \in \mathbb{Z}_{[0, M-1]}, e \in \mathcal{E}}$ . We measure  $u$  and  $y$ , which are both affected by the noise  $n$  due to the closed-loop setting.

The ease of performing data collection in such a closed-loop setting is, particularly, for unstable systems, an important benefit of considering frequency-domain data. Another benefit, which we will exploit next, is the fact that, in contrast with related results based on time-domain data, measuring more data in time domain does not lead to a higher computational

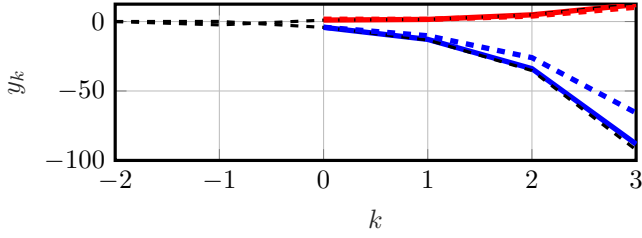


Fig. 3. Data-driven simulation of an unstable batch reactor using noisy data. We see that, using the data based on measuring  $p = 10$  periods, there is a significant error between the simulated output trajectories  $y_1$  (---) and  $y_2$  (---) and the true response (---). However, using the data based on measuring  $p = 50$  periods, leads to significantly more accurate simulations for  $y_1$  (—) and  $y_2$  (—).

complexity while it does allow the effect of noise to average out. We collect our data by measuring  $p + p_0$  periods of our multi-sine excitation, after which we discard the first  $p_0 = 20$  periods to eliminate most of the transient effects. This elementary method, which approximates measurements of the steady-state behavior [23], ensures that we (approximately) adhere to the conditions in Definition 3. To show the effect of measuring more periods, we collect data by measuring  $p = 10$  and  $p = 50$  periods. For each data set, we implement the data-driven simulation based on Proposition 1 using the same initial trajectory of length  $L_0 = \ell_\Sigma$  as in Example 2, and we simulate  $L = 4$  steps into the future using the same input sequence as in Example 2. The results are depicted in Fig. 3 along with the true output response of the system  $y_{[-L_0, L-1]}^{\text{true}}$ . We also carried out this data-driven simulation for a wider range of periods  $p$  and show the resulting absolute and relative errors in the simulated future outputs in Table I. As expected, we again see that the accuracy of the simulated future outputs improves significantly as the number of periods increases. Note that a significant error remains also for  $p = 50$ , especially towards the end of the simulated time window, because  $\Sigma$  with (9) is unstable and we are simulating the system in open loop. We emphasize that, when using frequency-domain data, doing so does not increase computational complexity because the dimensions of (7) and (8) do not scale with the number of periods  $p$  but rather with the number of excited frequencies  $M$ . As we will see in the next section, these computational benefits are particularly interesting when using Proposition 1 as the basis for a data-driven predictive control scheme, where computational cost is an important consideration due to the optimization that needs to be carried out in real time.

TABLE I  
ABSOLUTE AND RELATIVE ERROR IN SIMULATED FUTURE OUTPUT  
TRAJECTORY USING  $p$  PERIODS TO OBTAIN OFF-LINE DATA

	$\ y_{[0, L-1]} - y_{[0, L-1]}^{\text{true}}\ _2$	$\frac{\ y_{[0, L-1]} - y_{[0, L-1]}^{\text{true}}\ _2}{\ y_{[0, L-1]}^{\text{true}}\ _2}$
$p = 5$	$6.557 \cdot 10^1$	$6.506 \cdot 10^{-1}$
$p = 10$	$2.855 \cdot 10^1$	$2.833 \cdot 10^{-1}$
$p = 50$	7.6736	$7.614 \cdot 10^{-2}$
$p = 100$	5.378	$5.336 \cdot 10^{-2}$

## B. Data-driven frequency response evaluation

All the results presented so far mix time and frequency domain in the sense that they use frequency-domain off-line data to characterize the behavior of  $\Sigma$  in the time domain. For example, both of the frequency-domain versions of WFL, i.e., Theorem 1 and 2, feature a time-domain response of  $\Sigma$  on the left-hand side of Theorem 1.(ii) and Theorem 2.(ii), respectively, and frequency-domain data on the respective right-hand sides. Then, we utilize Theorem 2 to characterize the frequency-response of the system  $\Sigma$  at any complex frequency that does not coincide with an eigenvalue of  $A$ .

**Proposition 2:** Let  $\{(\hat{U}_{[0, M-1]}^e, \hat{Y}_{[0, M-1]}^e)\}_{e \in \mathcal{E}}$  be a collection of input-output spectra of  $\Sigma$  in (1) satisfying Assumption 1. Let  $L_0 \in \mathbb{Z}_{\geq \ell_\Sigma}$  and suppose that  $\{\hat{U}_{[0, M-1]}^e\}_{e \in \mathcal{E}}$  is CPE of order  $L_0 + 1 + n_x$ . Then, for any complex frequency  $z \in \mathbb{C}$  that is not an eigenvalue of  $A$  and a sample  $U_z \in \mathbb{C}^{n_u}$  of the input spectrum at  $z$ , the system of linear equations

$$\begin{bmatrix} 0 & \Psi_{L_0+1}(\{\hat{U}_{[0, M-1]}^e\}_{e \in \mathcal{E}}) \\ -W_{L_0+1}(z) \otimes I_{n_y} & \Psi_{L_0+1}(\{\hat{Y}_{[0, M-1]}^e\}_{e \in \mathcal{E}}) \end{bmatrix} \begin{bmatrix} Y_z \\ G \end{bmatrix} = \begin{bmatrix} W_{L_0+1}(z) \otimes U_z \\ 0 \end{bmatrix}, \quad (10)$$

where  $\Psi_{L_0+1}(\{\hat{U}_{[0, M-1]}^e\}_{e \in \mathcal{E}}) = \begin{bmatrix} \mathcal{F}_{L_0+1}(\{\hat{U}_{[0, M-1]}^e\}_{e \in \mathcal{E}}) & \mathcal{F}_{L_0+1}^*(\{\hat{U}_{[0, M-1]}^e\}_{e \in \mathcal{E}}) \end{bmatrix}$ , has a unique solution for  $Y_z$ , which is such that the complex-valued pair  $(U_z, Y_z)$  is a sample of the input-output spectrum of  $\Sigma$  at  $z$  (i.e.,  $Y_z = H(z)U_z$ ).

Proposition 2 allows us to evaluate the frequency response of  $\Sigma$  to an input “direction”  $U_z$  at the complex frequency  $z$ . Note that  $z$  does not necessarily have to correspond to any of the frequencies  $e^{j\omega_k}$ ,  $k \in \mathbb{Z}_{[0, M-1]}$ , present in our off-line data. In fact,  $z$  does not even have to be on the unit circle. Interestingly, if we take  $U_z$  to be the identity matrix and apply Proposition 2 to each of its columns individually, we can compute  $Y_z = H(z)$  and, thereby, we can compute the transfer function (matrix) of  $\Sigma$  at  $z$ . In fact, in this case, Proposition 2 recovers a version of [27, Theorem 2] that is using frequency-domain data. Importantly, unlike in the other results throughout this paper,  $G$  in Proposition 2 is not constrained to have a complex-conjugate structure (i.e.,  $(G_0, G_1, G_1^*)$  in, e.g., Theorem 1.(ii)). This is because the right-hand side of (10) is complex-valued.

## C. Frequency-domain data-driven LQR

In this section, we use Theorem 1 to perform a frequency-domain data-based LQR using input-state data, i.e., frequency-domain data consisting of input-state spectra. To be precise, we aim to design the optimal control law

$$u_k = Kx_k, \quad (11)$$

for the system  $\Sigma$  in (1) such that  $\lim_{k \rightarrow \infty} x_k = 0$ , and such that the cost function

$$J(\{x_k\}_{k \in \mathbb{Z}_{\geq 0}}, \{u_k\}_{k \in \mathbb{Z}_{\geq 0}}) = \sum_{k \in \mathbb{Z}_{\geq 0}} x_k^\top Q x_k + u_k^\top R u_k, \quad (12)$$



is minimized. In (12),  $Q \in \mathbb{R}^{n_x \times n_x}$  is symmetric positive semi-definite and  $R \in \mathbb{R}^{n_u \times n_u}$  is symmetric positive definite.

*Proposition 3:* Let  $\{\{\hat{U}_{[0,M-1]}^e, \hat{X}_{[0,M-1]}^e\}_{e \in \mathcal{E}}\}$  be a collection of input-state spectra of  $\Sigma$  in (1) satisfying Assumption 1. Suppose that  $\{\hat{U}_{[0,M-1]}^e\}_{e \in \mathcal{E}}$  is CPE of order  $n_x + 1$  and that every eigenvalue of  $A$  on the unit circle is  $(Q, A)$ -observable, i.e.,  $\text{rank}[Q \quad \lambda I - A] = n_x$  for all  $\lambda \in \mathbb{C}$  with  $|\lambda| = 1$ . Let

$$\Delta := \begin{bmatrix} X_0 \\ X_1 \\ \vdots \\ \hat{U} \end{bmatrix} := \begin{bmatrix} \mathcal{F}_2(\{\hat{X}_{[0,M-1]}^e\}_{e \in \mathcal{E}}) & \mathcal{F}_2^*(\{\hat{X}_{[1,M-1]}^e\}_{e \in \mathcal{E}}) \\ \mathcal{F}_1(\{\hat{U}_{[0,M-1]}^e\}_{e \in \mathcal{E}}) & \mathcal{F}_1^*(\{\hat{U}_{[1,M-1]}^e\}_{e \in \mathcal{E}}) \end{bmatrix},$$

and let  $\Psi(P) := \text{diag}\{Q - P, P, R\}$ . Then, there exists a right inverse  $X_0^\dagger$  of  $X_0$ , which is such that  $\Delta^H \Psi(P) \Delta X_0^\dagger = 0$  and such that the optimal control law that minimizes the cost (12) and achieves  $\lim_{k \rightarrow \infty} x_k = 0$  is given by (11) and

$$K = UX_0^\dagger, \quad (13)$$

where  $P$  is the unique solution to

$$\begin{aligned} \max_{P \in \mathbb{R}^{n_x \times n_x}} \quad & \text{trace } P \\ \text{s. t.} \quad & \Delta^H \Psi(P) \Delta \succcurlyeq 0, \quad P = P^\top \succcurlyeq 0. \end{aligned} \quad (14)$$

Proposition 3 presents what is essentially a frequency-domain version of [44, Theorem 29], but we assume that our off-line data is persistently exciting instead of using the informativity approach. The right inverse  $X_0^\dagger$  in (13) is not necessarily unique, but we can construct one as in (15) below.

*Example 4 (FRF-based LQR):* Consider again the unstable batch reactor given by (1) with  $A$  and  $B$  as in (9), but with full state measurements, i.e.,  $C = I$  and  $D = 0$ . We again generate our off-line frequency-domain data for the  $M = 10$  frequencies  $\hat{\omega}_{[0,M-1]}$  in (4) as outlined in Example 2. We use Proposition 3 to compute the LQR based on the resulting input-state spectra  $\{\{\hat{U}_{[0,M-1]}^e, \hat{X}_{[0,M-1]}^e\}_{e \in \mathcal{E}}\}$ . In particular, we minimize the cost function (12) with  $Q = I$  and  $R = I$  by, first, solving (14) to obtain  $P$  and, subsequently, computing  $K$  as in (13) with

$$X_0^\dagger = (\Delta^H \Psi(P) \Delta)_\perp (X_0 (\Delta^H \Psi(P) \Delta)_\perp)^+. \quad (15)$$

Observe that  $X_0^\dagger$  is, indeed, a right inverse of  $X_0$  while also satisfying  $\Delta^H \Psi(P) \Delta X_0^\dagger = 0$ . We find that

$$P = \begin{bmatrix} 3.6042 & 0.0490 & 1.7622 & -1.3063 \\ 0.0490 & 1.1700 & 0.0724 & 0.1416 \\ 1.7622 & 0.0724 & 2.2018 & -0.8446 \\ -1.3063 & 0.1416 & -0.8446 & 1.8234 \end{bmatrix},$$

$$K = \begin{bmatrix} 0.1626 & -0.2920 & 0.0495 & -0.3284 \\ 1.4183 & 0.1155 & 0.9841 & -0.6247 \end{bmatrix}.$$

Importantly and as expected based on Proposition 3, these results closely resemble the true solution  $\bar{P}$  to the discrete algebraic Riccati equation (DARE) and the corresponding LQR gain  $\bar{K}$ . In fact, we find that  $\|\bar{P} - P\|_2 = 1.7470 \cdot 10^{-9}$ ,  $\|\bar{P} - P\|_2 / \|\bar{P}\|_2 = 3.1972 \cdot 10^{-10}$ ,  $\|\bar{K} - K\|_2 = 4.6630 \cdot 10^{-11}$ , and  $\|\bar{K} - K\|_2 / \|\bar{K}\|_2 = 2.5117 \cdot 10^{-10}$ .

## VI. FREQUENCY-DOMAIN DATA-DRIVEN PREDICTIVE CONTROL

In Section V, we have already seen how Theorem 1 and Theorem 2 can be used to simulate the unknown system  $\Sigma$  in (1) based on frequency-domain data. Naturally, we can also use these results as a frequency-domain data-driven substitute for the prediction model in model predictive control (MPC). The resulting frequency-domain data-driven predictive control (FreePC) scheme, presented below, is the frequency-domain counterpart of DeePC [11].

### A. FreePC algorithm

Let  $T \in \mathbb{Z}_{\geq 1}$  be the length of the prediction horizon. We recall from Section V-A that we need to use a past input-output sequence to ensure that our simulation, which we refer to as our prediction in the context of FreePC, starts from the correct initial condition. Let  $\bar{T} \in \mathbb{Z}_{\geq \ell_\Sigma}$  denote the length of this past input-output sequence. Suppose we are given frequency-domain data consisting of the collection of  $E$  input-output spectra  $\{\{\hat{U}_{[0,M-1]}^e, \hat{Y}_{[0,M-1]}^e\}_{e \in \mathcal{E}}\}$  with  $\{\hat{U}_{[0,M-1]}^e\}_{e \in \mathcal{E}}$  being PE of order  $\bar{T} + T + n_x$ . Note that this implies that  $E(2M - 1) \geq \bar{T} + T + n_x \geq \ell_\Sigma + T + n_x$ .

At every time  $k \in \mathbb{Z}$ , given the past input-output sequence  $(u_{[k-\bar{T},k-1]}, y_{[k-\bar{T},k-1]})$ , the FreePC solution is now defined by solving the finite-horizon optimal control problem

$$\begin{aligned} \min_{\substack{u_{[0,T-1],k}, \\ y_{[0,T-1],k}, \\ G_{0,k}, G_{1,k}, \sigma_k}} \quad & \lambda_\sigma \|\sigma_k\|_1 + \lambda_G \|G_k\|_1 + \sum_{i \in \mathbb{Z}_{[0,T-1]}} \ell(y_{i,k}, u_{i,k}), \\ \text{s. t.} \quad & \begin{bmatrix} u_{[k-\bar{T},k-1]} \\ \dots \\ u_{[0,T-1],k} \\ y_{[k-\bar{T},k-1]} + \sigma_k \\ y_{[0,T-1],k} \end{bmatrix} = \\ & \begin{bmatrix} \mathcal{F}_{\bar{T}+T}(\{\hat{U}_{[0,M-1]}^e\}_{e \in \mathcal{E}}) & \mathcal{F}_{\bar{T}+T}^*(\{\hat{U}_{[1,M-1]}^e\}_{e \in \mathcal{E}}) \\ \mathcal{F}_{\bar{T}+T}(\{\hat{Y}_{[0,M-1]}^e\}_{e \in \mathcal{E}}) & \mathcal{F}_{\bar{T}+T}^*(\{\hat{Y}_{[1,M-1]}^e\}_{e \in \mathcal{E}}) \end{bmatrix} G_k, \\ & G_k = \begin{bmatrix} G_{0,k} \\ \dots \\ G_{1,k} \\ G_{1,k}^* \end{bmatrix}, \quad \text{with } G_{0,k} \in \mathbb{R}^E, G_{1,k} \in \mathbb{C}^{E(M-1)}, \\ & u_{i,k} \in \mathbb{U}, y_{i,k} \in \mathbb{Y}, \quad \text{for all } i \in \mathbb{Z}_{[0,T-1]}. \end{aligned} \quad (16)$$

Let  $u_{[0,T-1],k} = \{u_{i,k}^*\}_{i \in \mathbb{Z}_{[0,T-1]}}$  denote the optimal control action computed at time  $k \in \mathbb{Z}$  by solving (16). After solving (16), we implement the first element of the optimal control action  $u_{[0,T-1],k}^*$ , i.e.,  $u_k = u_{0,k}^*$  and, at time  $k + 1$ , we solve (16) again using the newly-obtained past input-output trajectory  $(u_{[k-\bar{T}+1,k]}, y_{[k-\bar{T}+1,k]})$ . This way, the optimal control is computed iteratively using the receding-horizon principle and a feedback policy is created.

We recall that  $u_{[0,T-1],k}$  and  $y_{[0,T-1],k}$  denote the (vectorized) sequence of predictions of  $u_{k+i}$  and  $y_{k+i}$ ,  $i \in \mathbb{Z}_{[0,T-1]}$ , respectively, as introduced in Section II-D. Moreover, similar to DeePC,  $\ell$  denotes the stage cost,  $\mathbb{U}$  and  $\mathbb{Y}$  denote, respectively, the sets of admissible inputs and outputs,  $\sigma_k \in \mathbb{R}^{\bar{T}n_y}$  is an auxiliary slack variable, and  $\lambda_\sigma, \lambda_G \in \mathbb{R}_{>0}$  are regularization parameters. The slack variable and the regularization parameters are needed to deal with noise in  $y_{[k-\bar{T},k-1]}$  and

in the data  $\{(\hat{U}_{[0,M-1]}^e, \hat{Y}_{[0,M-1]}^e)\}_{e \in \mathcal{E}}$ . Some further remarks regarding the optimization problem in (16) are in order.

- The prediction model in (16) involves the product between a complex-valued matrix and vector. Importantly,  $G_{0,k} \in \mathbb{R}^E$  is real and  $G_{1,k} \in \mathbb{C}^{E(M-1)}$  is complex, and the conjugate symmetry in (16) ensures that the left-hand side of the prediction model is always real-valued. Depending on the solver that is being used, however, it is often beneficial to apply the change of variables involving  $T_{\Re}$ , as described in Section IV-B, to obtain a real-valued formulation that is equivalent to (16).
- In DeePC, the number of decision variables, through  $g_k \in \mathbb{R}^{N-\bar{T}-T+1}$  in (3), depends on the length  $N$  of the time-domain data. Interestingly, in FreePC, the number of decision variables, through  $G_{0,k}$  and  $G_{1,k}$  in (16), depends only on the number of frequencies  $M$  and experiments  $E$  and not on the length of the time-domain data used to compute  $(\hat{U}_{[0,M-1]}^e, \hat{Y}_{[0,M-1]}^e)$ . As we saw in Example 3 and will further illustrate in Section VI-C, we can exploit this to perform longer experiments and, thereby, reduce the effect of noise *without* increasing the computational complexity of FreePC.

### B. An equivalence result

Interestingly, when  $\lambda_g = 0$  in (3) and  $\lambda_G = 0$  in (16), which is possible when the off-line data is noise-free, we can show that FreePC is equivalent to DeePC.

*Theorem 3:* Let  $\{(\hat{U}_{[0,M-1]}^e, \hat{Y}_{[0,M-1]}^e)\}_{e \in \mathcal{E}}$  and  $(\hat{u}_{[0,N-1]}, \hat{y}_{[0,N-1]})$  be, respectively, a collection input-output spectra and a trajectory of  $\Sigma$  in (1) satisfying Assumption 1. Let  $\bar{T} \in \mathbb{Z}_{\geq \ell_{\Sigma}}$  and  $T \in \mathbb{Z}_{\geq 1}$  and suppose that  $\{\hat{U}_{[0,M-1]}^e\}_{e \in \mathcal{E}}$  and  $\hat{u}_{[0,N-1]}$  are PE of order  $\bar{T} + T + n_x$ . Suppose that  $\{(\hat{U}_{[0,M-1]}^e, \hat{Y}_{[0,M-1]}^e)\}_{e \in \mathcal{E}}$  and  $(\hat{u}_{[0,N-1]}, \hat{y}_{[0,N-1]})$  are noise-free and, accordingly, set  $\lambda_g = 0$  in (3) and  $\lambda_G = 0$  in (16). Let  $(u_{[k-\bar{T},k-1]}, y_{[k-\bar{T},k-1]})$  be the past input-output trajectory available at time  $k \in \mathbb{Z}$ . Then, FreePC based on (16) is equivalent to DeePC based on (3) in the sense that, at any  $k \in \mathbb{Z}$ , the open-loop optimal control problems in (16) and (3) admit the same (set of) optimal control action(s) and corresponding output sequence(s).

It immediately follows from Theorem 3 that, if (3) admits a unique optimal control action  $u_{0,k}^*$ , then  $u_{0,k}^*$  is also the unique optimal control action obtained by solving (16) and vice versa. Theorem 3 considers FreePC based on *multiple* experiments and DeePC based on *a single* experiment, however, a similar equivalence holds for DeePC based on multiple experiments.

### C. Numerical case study

Consider the unstable SISO system  $\Sigma$  of the form (1) with transfer function

$$H(z) = \frac{0.1164z + 0.1071}{z^2 - 1.891z + 0.7788}. \quad (17)$$

While we consider a SISO example here because it allows us to illustrate and visualize our results more easily, we note that the FreePC scheme as introduced in Section VI also applies

to MIMO systems. To incorporate the effect of noise in our case study, we replace the measurement model in (1b) with

$$y_k = Cx_k + Du_k + n_k$$

to incorporate measurements noise. Since the system (17) is unstable, we collect our off-line data in a closed-loop measurement setup [25, Chapter 10], as depicted in Fig. 2, with the stabilizing controller  $C(z) = (6z - 5.135)/(z - 0.1353)$ . The input  $u_k \in \mathbb{R}$  consists of the output of the controller on top of which we inject a signal  $\{d_k\}_{k \in \mathbb{Z}}$  with  $d_k \in \mathbb{R}$  for all  $k \in \mathbb{Z}$ , as seen in Fig. 2. As mentioned before, the ease of performing data collection in such a closed-loop setting is, particularly, for unstable systems, an important benefit of considering frequency-domain data.

We generate off-line data using a multi-sine excitation for the injected signal  $\{d_k\}_{k \in \mathbb{Z}}$ , which contains the  $M = 20$  frequencies  $\hat{\omega}_{[0,M-1]}$  in (4), and zero-mean Gaussian noise  $n_k$  with a standard deviation of 0.1. We measure  $p + p_0$  periods of  $d_k$ ,  $u_k$  and  $y_k$  at the excited frequencies and, subsequently, discard the first  $p_0$  periods in order to get rid of most transient phenomena. Then, we compute *per period* the DTFT to obtain  $\{\hat{D}_{\rho}^d(\hat{\omega}_k)\}_{\rho \in \mathcal{P}, k \in \mathbb{Z}_{[0,M-1]}}$ ,  $\{\hat{U}_{\rho}^d(\hat{\omega}_k)\}_{\rho \in \mathcal{P}, k \in \mathbb{Z}_{[0,M-1]}}$  and  $\{\hat{Y}_{\rho}^d(\hat{\omega}_k)\}_{\rho \in \mathcal{P}, k \in \mathbb{Z}_{[0,M-1]}}$  with  $\mathcal{P} := \mathbb{Z}_{[1,p]}$ . Instead of using this data directly, we will now estimate the transfer function at the frequencies  $\hat{\omega}_{[0,M-1]}$  such that we can illustrate how the accuracy of the data improves with measuring more periods. Using that (assuming no transient phenomena and noise),

$$\begin{aligned} \hat{U}_{\rho}^d(\hat{\omega}_k) &= (1 - C(e^{j\hat{\omega}_k})G(e^{j\hat{\omega}_k}))^{-1} \hat{D}_{\rho}^d(\hat{\omega}_k), \\ \hat{Y}_{\rho}^d(\hat{\omega}_k) &= G(e^{j\hat{\omega}_k}) \hat{U}_{\rho}^d(\hat{\omega}_k), \end{aligned}$$

for  $m \in \mathbb{Z}_{[0,M-1]}$  and  $\rho \in \mathcal{P}$ , we estimate, for each measured period, the transfer function at  $\hat{\omega}_k$  by

$$\hat{H}_{\rho}(\hat{\omega}_k) = \frac{\hat{Y}_{\rho}^d(\hat{\omega}_k)(\hat{D}_{\rho}^d(\hat{\omega}_k))^*}{\hat{U}_{\rho}^d(\hat{\omega}_k)(\hat{D}_{\rho}^d(\hat{\omega}_k))^*}.$$

Averaging over all periods yields our estimated FRF, which is the sample mean, i.e.,

$$\hat{H}(e^{j\hat{\omega}_k}) = \frac{1}{p} \sum_{\rho \in \mathcal{P}} \hat{H}_{\rho}(\hat{\omega}_k).$$

To characterize the uncertainty in our estimated FRF, we also compute the sample variance of  $\hat{H}(\hat{\omega}_k)$  according to<sup>3</sup>

$$\text{var } \hat{H}(e^{j\hat{\omega}_k}) = \frac{1}{p(p-1)} \sum_{\rho \in \mathcal{P}} |\hat{H}_{\rho}(\hat{\omega}_k) - \hat{H}(\hat{\omega}_k)|^2.$$

Figure 4 shows the resulting FRF measurements along with their 99% confidence intervals (computed according to [45, Chapter 6]) using  $p = 2$  and  $p = 50$  periods. It is worth mentioning that the ability to visualize and intuitively interpret the confidence intervals, as we have done in Fig. 4, is another important benefit of working with frequency-domain data. From Fig. 4, we observe that the confidence intervals for  $p = 50$  shrink (except at the high frequencies) significantly compared to  $p = 2$ . The lower variance is also reflected in

<sup>3</sup>While more advanced methods exist to estimate FRFs and their variances, see, e.g., [23], this approach suffices to illustrate our results.

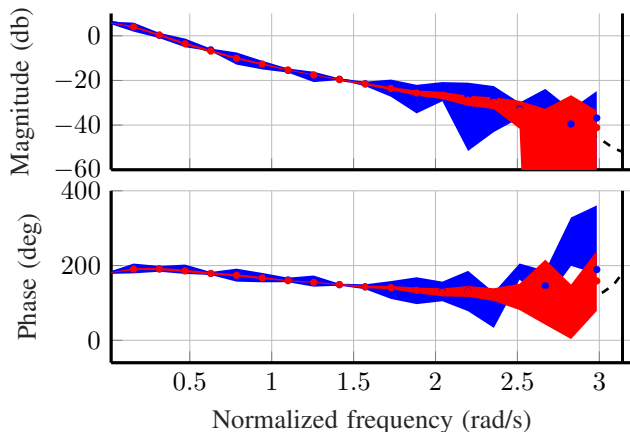


Fig. 4. Estimated FRF of the system ( $\bullet\text{-}\bullet$ ) using  $p = 2$  ( $\bullet$ ) and  $p = 50$  periods ( $\bullet$ ) with their respective 99% confidence intervals ( $\square$  /  $\square$ ).

the accuracy of the FRF measurements, which is better for  $p = 50$  compared to  $p = 2$ . This is not surprising because measuring more periods means that the effect of the random noise is averaged out more, which results in more accurate estimates. Interestingly, in DeePC measuring more periods would result in a higher number of decision variables and, thereby, higher (on-line) computational complexity, but, as mentioned before, the computational complexity of FreePC is independent of the time-domain experiment duration and, instead, depends on the number of excited frequencies. This illustrates an important advantage that many techniques based on our frequency-domain WFL, such as FreePC, have over their time-domain counterparts.

Next, we implement FreePC based on the obtained FRF measurements. Since we are dealing with a SISO system, we use  $E = 1$ . Let  $\hat{U}_k = 1$  and  $\hat{Y}_k = \hat{H}(e^{j\hat{\omega}_k})$  for all  $k \in \mathbb{Z}_{[0, M-1]}$ . Let the prediction horizon be  $T = 10$ , and we take the initial input-output trajectory to be of length  $\bar{T} = 3n_x = 6 \geq \ell_\Sigma$ . It is straightforward to verify that  $\hat{U}_{[0, M-1]}$  is PE of order  $2M - 1 = 39 \geq T + \bar{T} + n_x = 18$ . Moreover, we use the stage cost  $\ell(y, u) = y^\top Qy + u^\top Ru$  with  $Q = 1$  and  $R = 0.01$  and regularization parameters  $\lambda_G = 0.1$  and  $\lambda_\sigma = 1 \cdot 10^5$ . The sets of admissible inputs and outputs are given, respectively, by  $\mathbb{U} = [-3, 0.5]$  and  $\mathbb{Y} = [-0.5, 1.2]$ . We simulate the resulting FreePC scheme based on the two sets of FRF measurements in Fig. 4, which were obtained by measuring  $p = 2$  and  $p = 50$  periods. The resulting input and output trajectories are depicted in Fig. 5. As expected, we observe that the FreePC scheme based on  $p = 50$  periods performs better than the one with  $p = 2$ . In fact, it closely resembles the input-output trajectories obtained using a model-based benchmark, i.e., a similarly tuned MPC scheme (based on the exact model), that are also shown in Fig. 5. To further

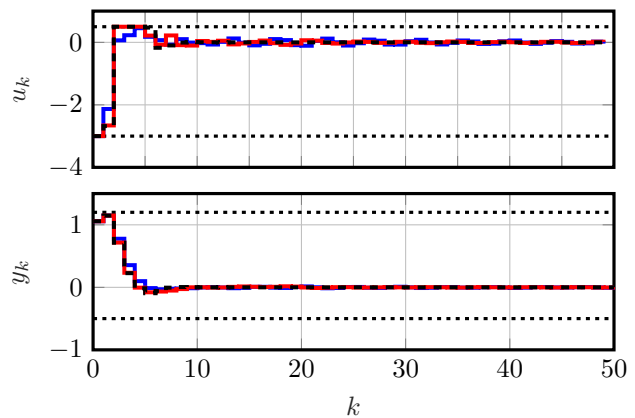


Fig. 5. Simulation, with constraints ( $\cdots$ ), of FreePC using data with 2 ( $\text{---}$ ) and 50 ( $\text{---}$ ) periods, and an MPC benchmark ( $\text{---}$ ).

investigate the relation between the number of periods and the achieved performance, we perform a Monte Carlo study, in which we implement FreePC based on data sets generated as discussed before. We consider data sets containing  $p = \{5, 10, 25, 50\}$  periods (after we have again discarded the first 20 periods to eliminate most transient phenomena), for which we compute the obtained cost as

$$J = \sum_{k \in \mathbb{Z}_{[0, L_{\text{sim}}-1]}} \ell(y_k, u_k),$$

throughout the duration  $L_{\text{sim}} = 50$  of the simulation. The average cost and the variance of the cost throughout 1000 runs are recorded in Table II along with the cost of the model-based benchmark. Since the FRF measurements become more representative of the true system (17) as the number of periods increases, the average achieved cost and its variance decrease for higher  $p$ , which can, indeed, be seen in Table II. This shows that FreePC has similar (performance) properties as a classical MPC using a parametric state-space prediction model, provided that the obtained FRF data is sufficiently accurate.

## VII. CONCLUSIONS

In this paper, we presented a novel version of Willems' fundamental lemma based on frequency-domain data, which can be used to fully characterize the input-output behavior of an unknown (possibly unstable) system. In doing so, we also provided a definition of persistence of excitation for frequency-domain data, and we presented extensions of these results to accommodate multiple data sets. To show the potential impact of these new results, we demonstrate their application to data-driven simulation, frequency response evaluation (at other frequencies than available in the off-line data), and data-driven LQR. We also used the frequency-domain fundamental lemma to present a novel data-driven predictive control scheme, called FreePC, that utilizes frequency-domain data *without* the need to convert it into a parametric (state-space) model. Thereby, we bridge the gap between recent advances in data-driven analysis and (predictive) control and existing tools and expertise on frequency-domain control/identification in academia and industry. Numerical results are also presented

TABLE II  
MONTE CARLO STUDY OF FREEPC USING 1000 DATA SETS CONTAINING  $p$  PERIODS.

	MPC benchmark	$p = 5$	$p = 10$	$p = 25$	$p = 50$
Mean $J$	3.1801	3.2620	3.2204	3.1912	3.1873

in which we illustrate several benefits of using frequency-domain data particularly when dealing with noisy data.

## APPENDIX

### A. Proof of Theorem 1

Let  $(\hat{U}_{[0,M-1]}, \hat{X}_{[0,M-1]}, \hat{Y}_{[0,M-1]})$  be an input-state-output spectrum of  $\Sigma$  in (1) satisfying Assumption 1. Suppose that  $\hat{U}_{[0,M-1]}$  is PE of order  $L + n_x$ .

1) *Proof of statement (i)*: To show that statement (i) holds, it suffices to show that, for any  $b \in \mathbb{C}^{n_x + n_u L}$ ,

$$b^H \begin{bmatrix} F_1(\hat{X}_{[0,M-1]}) & F_1^*(\hat{X}_{[1,M-1]}) \\ F_L(\hat{U}_{[0,M-1]}) & F_L^*(\hat{U}_{[1,M-1]}) \end{bmatrix} = 0 \implies b = 0. \quad (18)$$

To this end, we write  $b = (\xi, \eta)$  with  $\xi \in \mathbb{C}^{n_x}$  and  $\eta \in \mathbb{C}^{n_u L}$  such that the left equality in (18) holds. Define  $b_0 := (\xi, \eta, 0_{n_x n_u})$ . From (18), we get

$$b_0^H \underbrace{\begin{bmatrix} F_1(\hat{X}_{[0,M-1]}) & F_1^*(\hat{X}_{[1,M-1]}) \\ F_{L+n_x}(\hat{U}_{[0,M-1]}) & F_{L+n_x}^*(\hat{U}_{[1,M-1]}) \end{bmatrix}}_{=:\Theta \in \mathbb{C}^{(n_x + (L+n_x)n_u) \times (2M-1)}} = 0. \quad (19)$$

Next, we introduce the matrix

$$\Lambda := \text{diag}\{1, e^{j\hat{\omega}_1}, \dots, e^{j\hat{\omega}_{M-1}}, e^{-j\hat{\omega}_1}, \dots, e^{-j\hat{\omega}_{M-1}}\}.$$

Then, from (19), it immediately holds that  $b_0^H \Theta \Lambda = 0$ . Let  $\hat{X}_k^+ := e^{j\hat{\omega}_k} \hat{X}_k$  and  $\hat{U}_k^+ := e^{j\hat{\omega}_k} \hat{U}_k$  for all  $k \in \mathbb{Z}_{[0,M-1]}$ . It follows that

$$\begin{aligned} 0 &= b_0^H \Theta \Lambda = b_0^H \begin{bmatrix} F_1(\hat{X}_{[0,M-1]}^+) & F_1^*(\hat{X}_{[1,M-1]}^+) \\ F_{L+n_x}(\hat{U}_{[0,M-1]}^+) & F_{L+n_x}^*(\hat{U}_{[1,M-1]}^+) \end{bmatrix}, \\ \stackrel{(5a)}{=} &\begin{bmatrix} A^\top \xi \\ B^\top \xi \\ \eta \\ 0_{(n_x-1)n_u} \end{bmatrix}^H \begin{bmatrix} F_1(\hat{X}_{[0,M-1]}) & F_1^*(\hat{X}_{[1,M-1]}) \\ F_{L+n_x}(\hat{U}_{[0,M-1]}) & F_{L+n_x}^*(\hat{U}_{[1,M-1]}) \end{bmatrix}, \end{aligned}$$

where we exploit the specific structure of  $F_1(\hat{X}_{[0,M-1]})$  and  $F_{L+n_x}(\hat{U}_{[0,M-1]})$ , defined in (6). Repeating this process yields that, for any  $m \in \mathbb{Z}_{[0,n_x]}$ ,

$$\begin{aligned} 0 &= b_0^H \Theta \Lambda^m \stackrel{(5a)}{=} \\ &\underbrace{\begin{bmatrix} \xi^H A^m & \xi^H A^{m-1} B & \dots & \xi^H B & \eta^H & 0_{(n_x-m)n_u}^\top \end{bmatrix}}_{=: \bar{b}_m^H} \Theta. \end{aligned} \quad (20)$$

Since  $\hat{U}_{[0,M-1]}$  is PE of order  $L + n_x$ , the bottom  $(L + n_x)n_u$  rows of  $\Theta$  are linearly independent, i.e.,  $\begin{bmatrix} F_{L+n_x}(\hat{U}_{[0,M-1]}) & F_{L+n_x}^*(\hat{U}_{[1,M-1]}) \end{bmatrix}$  has full row rank being  $(L + n_x)n_u$ . Hence,  $\dim \ker \Theta^H = n_x + (L + n_x)n_u - \text{rank} \Theta \leq n_x$ , which means that the  $n_x + 1$  vectors  $b_m, m \in \mathbb{Z}_{[0,n_x]}$ , as defined in (20), must be linearly dependent. We can

deduce that  $\eta = 0$  as follows: We write  $\eta = (\eta_1, \eta_2, \dots, \eta_L)$  with  $\eta_i \in \mathbb{C}^{n_u}$  for  $i \in \mathbb{Z}_{[1,L]}$ . If  $\eta_L \neq 0$ , then the matrix

$$[b_0 \ b_1 \ \dots \ b_{n_x}] = \begin{bmatrix} \xi & A^\top \xi & \dots & (A^{n_x})^\top \xi \\ \eta_1 & B^\top \xi & \dots & (A^{n_x-1} B)^\top \xi \\ \eta_2 & \eta_1 & \dots & (A^{n_x-2} B)^\top \xi \\ \vdots & \vdots & \ddots & \vdots \\ \eta_{L-1} & \eta_{L-2} & \dots & \beta_{L-1}(\xi, \eta) \\ \eta_L & \eta_{L-1} & \dots & \beta_L(\xi, \eta) \\ 0 & \eta_L & \dots & \beta_{L+1}(\xi, \eta) \\ \vdots & \vdots & \ddots & \vdots \\ 0 & 0 & \dots & \eta_{L-1} \\ 0 & 0 & \dots & \eta_L \end{bmatrix}, \quad (21)$$

with

$$\beta_\lambda(\xi, \eta) = \begin{cases} (A^{n_x-\lambda} B)^\top \xi, & \text{if } \lambda \leq n_x, \\ \eta_{\lambda-L}, & \text{if } \lambda > n_x, \end{cases}$$

would have full column rank, which contradicts the linear dependence of the vectors  $b_m, m \in \mathbb{Z}_{[0,n_x]}$ . Hence, it must hold that  $\eta_L = 0$ . After substituting  $\eta_L = 0$  in (21), we see that, if  $\eta_{L-1} \neq 0$ , the matrix in (21) again would have full column rank, which contradicts with the linear dependence of the vectors  $b_m, m \in \mathbb{Z}_{[0,n_x]}$ . Hence, it must also hold that  $\eta_{L-1} = 0$ . Repeating this process  $L$  times yields  $\eta = 0$ .

By the Cayley-Hamilton theorem, there exist  $c_i \in \mathbb{R}, i \in \mathbb{Z}_{[0,n_x-1]}$ , such that  $A^{n_x} = \sum_{n \in \mathbb{Z}_{[0,n_x-1]}} c_n A^n$ . It follows that

$$\begin{aligned} \bar{b} &= b_{n_x} - \sum_{n \in \mathbb{Z}_{[0,n_x-1]}} c_n b_n \\ &= \begin{bmatrix} 0_{n_x \times n_x} \\ B^\top (A^{n_x-1} - c_{n_x-1} A^{n_x-2} - \dots - c_1 I_{n_x})^\top \\ B^\top (A^{n_x-2} - c_{n_x-1} A^{n_x-3} - \dots - c_2 I_{n_x})^\top \\ \vdots \\ B^\top (A - c_{n_x-1} I_{n_x})^\top \\ B^\top \\ 0_{n_u L \times n_x} \end{bmatrix} \xi. \end{aligned}$$

Since  $\bar{b}$  is a linear combination of the vectors  $b_m, m \in \mathbb{Z}_{[0,n_x]}$ , it holds that  $\bar{b}^H \Theta = 0$ . However, due to PE, the bottom  $L + n_x$  rows of  $\Theta$  are full row rank and, thus,  $\bar{b} = 0$ . It follows that  $B^\top \xi = 0$ , which we substitute in the row above to find  $B^\top (A - c_{n_x} I_{n_x})^\top \xi = B^\top A^\top \xi = 0$ . Repeating this process yields  $B^\top (A^{n_x-1} - c_{n_x-1} A^{n_x-2} - \dots - c_1 I_{n_x})^\top \xi = B^\top (A^{n_x-1})^\top \xi = 0$ , which, due to Assumption 1, means that  $\xi = 0$ . Thus, we can conclude that  $b_0 = 0$ . It follows that (18) indeed holds, and, thereby, statement (i) holds.

2) *Proof of statement (ii)*: By applying (1) repeatedly, the pair of real-valued sequences  $(u_{[0,L-1]}, y_{[0,L-1]})$  of length  $L$  is an input-output trajectory of  $\Sigma$  if and only if there exists  $x_0 \in \mathbb{R}^{n_x}$  such that

$$\begin{bmatrix} u_{[0,L-1]} \\ y_{[0,L-1]} \end{bmatrix} = \begin{bmatrix} 0 & I \\ \mathcal{O}_L & \mathcal{T}_L \end{bmatrix} \begin{bmatrix} x_0 \\ u_{[0,L-1]} \end{bmatrix}, \quad (22)$$

where  $\mathcal{O}_L$  is the observability matrix (2) and

$$\mathcal{T}_L := \begin{bmatrix} D & 0 & \dots & 0 & 0 \\ CB & D & \dots & 0 & 0 \\ \vdots & \vdots & \ddots & \ddots & \vdots \\ CA^{L-2}B & CA^{L-3}B & \dots & CB & D \end{bmatrix}. \quad (23)$$

Let

$$\Omega := \begin{bmatrix} F_1(\hat{X}_{[0,M-1]}) & F_1^*(\hat{X}_{[1,M-1]}) \\ F_L(\hat{U}_{[0,M-1]}) & F_L^*(\hat{U}_{[1,M-1]}) \end{bmatrix} (\star)^H,$$

which, by construction, is real-valued. Due to Theorem 1.(i), it follows that  $\Omega$  is positive definite and, thus, for any  $x_0 \in \mathbb{R}^{n_x}$  and  $u_{[0,L-1]} \in \mathbb{R}^{n_u L}$ , there exists  $g \in \mathbb{R}^{n_x + n_u L}$  such that

$$\begin{bmatrix} x_0 \\ u_{[0,L-1]} \end{bmatrix} = \Omega g.$$

It follows that

$$G := \begin{bmatrix} G_0 \\ G_1 \\ G_2 \end{bmatrix} := \begin{bmatrix} F_1^H(\hat{X}_0) & F_L^H(\hat{U}_0) \\ \hline F_1^H(\hat{X}_{[1,M-1]}) & F_L^H(\hat{U}_{[1,M-1]}) \\ F_1^\top(\hat{X}_{[1,M-1]}) & F_L^\top(\hat{U}_{[1,M-1]}) \end{bmatrix} g, \quad (24)$$

where  $G_0 \in \mathbb{C}$  and  $G_1, G_2 \in \mathbb{C}^{2(M-1)}$ , satisfies

$$\begin{bmatrix} x_0 \\ u_{[0,L-1]} \end{bmatrix} = \begin{bmatrix} F_1(\hat{X}_{[0,M-1]}) & F_1^*(\hat{X}_{[1,M-1]}) \\ F_L(\hat{U}_{[0,M-1]}) & F_L^*(\hat{U}_{[1,M-1]}) \end{bmatrix} G. \quad (25)$$

Since  $F_1^H(\hat{X}_0)$ ,  $F_L^H(\hat{U}_0)$  and  $g$  are real, it follows from (24) that  $G_0 \in \mathbb{R}$ . By inspection of (24), we also conclude that  $G_1 = G_2^*$ . Observe that, by (5),  $\hat{U}_{[0,M-1]}$ ,  $\hat{X}_{[0,M-1]}$  and  $\hat{Y}_{[0,M-1]}$  satisfy, for all  $m \in \mathbb{Z}_{[0,M-1]}$ ,

$$W_L(e^{j\hat{\omega}}) \otimes \hat{Y}_m = \mathcal{O}_L \hat{X}_m + \mathcal{T}_L(W_L(e^{j\hat{\omega}m}) \otimes \hat{U}_m).$$

Thereby, it follows that

$$F_L(\hat{Y}_{[0,M-1]}) = \mathcal{O}_L F_1(\hat{X}_{[0,M-1]}) + \mathcal{T}_L F_L(\hat{U}_{[0,M-1]}).$$

Hence, substituting (25) into (22) yields statement (ii).

### B. Sketch of proof for Theorem 2

Let  $\{(\hat{U}_{[0,M-1]}^e, \hat{X}_{[0,M-1]}^e, \hat{Y}_{[0,M-1]}^e)\}_{e \in \mathcal{E}}$  be a collection of input-state-output spectra of  $\Sigma$  in (1) satisfying Assumption 1. Suppose that  $\{\hat{U}_{[0,M-1]}^e\}_{e \in \mathcal{E}}$  is CPE of order  $L + n_x$ .

1) *Sketch of proof for statement (i):* Similar to the proof of Theorem 1.(i), it suffices to show that, for any  $b \in \mathbb{C}^{n_x + n_u L}$ ,

$$b^H \begin{bmatrix} \mathcal{F}_1(\{\hat{X}_{[0,M-1]}^e\}_{e \in \mathcal{E}}) & \mathcal{F}_1^*(\{\hat{X}_{[1,M-1]}^e\}_{e \in \mathcal{E}}) \\ \mathcal{F}_L(\{\hat{U}_{[0,M-1]}^e\}_{e \in \mathcal{E}}) & \mathcal{F}_L^*(\{\hat{U}_{[1,M-1]}^e\}_{e \in \mathcal{E}}) \end{bmatrix} = 0$$

implies that  $b = 0$ . To show this, we replace

$$\Theta := \begin{bmatrix} \mathcal{F}_1(\{\hat{X}_{[0,M-1]}^e\}_{e \in \mathcal{E}}) & \mathcal{F}_1^*(\{\hat{X}_{[1,M-1]}^e\}_{e \in \mathcal{E}}) \\ \mathcal{F}_{L+n_x}(\{\hat{U}_{[0,M-1]}^e\}_{e \in \mathcal{E}}) & \mathcal{F}_{L+n_x}^*(\{\hat{U}_{[1,M-1]}^e\}_{e \in \mathcal{E}}) \end{bmatrix}$$

and  $\Lambda := \text{diag}\{I_E, \Lambda_1, \Lambda_1^*\}$ , with

$$\Lambda_1 = \text{diag}\{e^{j\hat{\omega}_1} I_E, \dots, e^{j\hat{\omega}_{M-1}} I_E\},$$

in the proof of Theorem 1.(i), after which the proof holds *mutatis mutandis*.

2) *Sketch of proof for statement (ii):* To prove Theorem 2.(ii), we replace

$$\Omega := \begin{bmatrix} \mathcal{F}_1(\{\hat{X}_{[0,M-1]}^e\}_{e \in \mathcal{E}}) & \mathcal{F}_1^*(\{\hat{X}_{[1,M-1]}^e\}_{e \in \mathcal{E}}) \\ \mathcal{F}_L(\{\hat{U}_{[0,M-1]}^e\}_{e \in \mathcal{E}}) & \mathcal{F}_L^*(\{\hat{U}_{[1,M-1]}^e\}_{e \in \mathcal{E}}) \end{bmatrix} (\star)^H,$$

in the proof of Theorem 1.(ii), after which the proof holds *mutatis mutandis*. To see this, note that

$$\begin{aligned} \mathcal{F}_L(\{\hat{Y}_{[0,M-1]}^e\}_{e \in \mathcal{E}}) &= \\ \mathcal{O}_L \mathcal{F}_1(\{\hat{X}_{[0,M-1]}^e\}_{e \in \mathcal{E}}) &+ \mathcal{T}_L \mathcal{F}_L(\{\hat{U}_{[0,M-1]}^e\}_{e \in \mathcal{E}}), \end{aligned}$$

with  $\mathcal{O}_L$  as in (2) and  $\mathcal{T}_L$  as in (23).

### C. Proof of Proposition 1

Let  $\{(\hat{U}_{[0,M-1]}^e, \hat{Y}_{[0,M-1]}^e)\}_{e \in \mathcal{E}}$  be a collection of input-output spectra of  $\Sigma$  in (1) satisfying Assumption 1. Let  $\{\hat{X}_{[0,M-1]}^e\}_{e \in \mathcal{E}}$  be the corresponding state spectra. Suppose that  $\{\hat{U}_{[0,M-1]}^e\}_{e \in \mathcal{E}}$  is CPE of order  $L + L_0 + n_x$ . For the past input-output trajectory  $(u_{[-L_0,-1]}, y_{[-L_0,-1]})$ , there exists  $x_{-L_0} \in \mathbb{R}^{n_x}$  such that

$$y_{[-L_0,-1]} = \mathcal{O}_{L_0} x_{-L_0} + \mathcal{T}_{L_0} u_{[-L_0,-1]}, \quad (26)$$

with  $\mathcal{O}_L$  as in (2) and  $\mathcal{T}_L$  as in (23). Due to CPE, by Theorem 2.(i), the matrix

$$\Omega_1 := \begin{bmatrix} \mathcal{F}_1(\{\hat{X}_{[0,M-1]}^e\}_{e \in \mathcal{E}}) & \mathcal{F}_1^*(\{\hat{X}_{[1,M-1]}^e\}_{e \in \mathcal{E}}) \\ \mathcal{F}_{L_0+L}(\{\hat{U}_{[0,M-1]}^e\}_{e \in \mathcal{E}}) & \mathcal{F}_{L_0+L}^*(\{\hat{U}_{[1,M-1]}^e\}_{e \in \mathcal{E}}) \end{bmatrix}$$

has full row rank and, thereby, the matrix  $\Omega_1 \Omega_1^H$  is positive definite. Since  $\Omega_1 \Omega_1^H$  is real by construction, it follows that, for any  $x_{-L_0} \in \mathbb{R}^{n_x}$  and  $u_{[-L_0,L-1]} \in \mathbb{R}^{n_u(L_0+L)}$ , there exists a  $g \in \mathbb{R}^{n_x + n_u(L_0+L)}$  such that

$$\begin{bmatrix} x_{-L_0} \\ u_{[-L_0,L-1]} \end{bmatrix} = \Omega_1 \Omega_1^H g. \quad (27)$$

Observe that, by (5), it holds that

$$\begin{bmatrix} \mathcal{O}_{L_0} & \mathcal{T}_{L_0} & 0_{n_y L_0 \times n_u L} \end{bmatrix} \Omega_1 = \begin{bmatrix} \mathcal{F}_{L_0}(\{\hat{Y}_{[0,M-1]}^e\}_{e \in \mathcal{E}}) & \mathcal{F}_{L_0}^*(\{\hat{Y}_{[1,M-1]}^e\}_{e \in \mathcal{E}}) \end{bmatrix}. \quad (28)$$

Combining (27) and (28) gives that  $G = \Omega_1^H g$  satisfies

$$\begin{aligned} \begin{bmatrix} u_{[-L_0,-1]} \\ u_{[0,L-1]} \\ u_{[-L_0,-1]} \end{bmatrix} &= \begin{bmatrix} 0 & I & 0 \\ 0 & 0 & I \\ \mathcal{O}_{L_0} & \mathcal{T}_{L_0} & 0 \end{bmatrix} \underbrace{\begin{bmatrix} x_{-L_0} \\ u_{[-L_0,-1]} \\ u_{[0,L-1]} \end{bmatrix}}_{\stackrel{(27)}{\Omega_1^H G}} \\ &= \begin{bmatrix} \mathcal{F}_{L_0+L}(\{\hat{U}_{[0,M-1]}^e\}_{e \in \mathcal{E}}) & \mathcal{F}_{L_0+L}^*(\{\hat{U}_{[1,M-1]}^e\}_{e \in \mathcal{E}}) \\ \mathcal{F}_{L_0}(\{\hat{Y}_{[0,M-1]}^e\}_{e \in \mathcal{E}}) & \mathcal{F}_{L_0}^*(\{\hat{Y}_{[1,M-1]}^e\}_{e \in \mathcal{E}}) \end{bmatrix} G, \end{aligned}$$

and  $G$  is of the form  $G = (G_0, G_1, G_1^*)$  with  $G_0 \in \mathbb{R}^E$  and  $G_1 \in \mathbb{C}^{E(M-1)}$ . This completes the first part of the proof.

The fact that  $(u_{[-L_0,L-1]}, y_{[-L_0,L-1]})$  with

$$\begin{aligned} y_{[-L_0,L-1]} &= \\ \mathcal{F}_{L_0+L}(\{\hat{Y}_{[0,M-1]}^e\}_{e \in \mathcal{E}}) & \mathcal{F}_{L_0+L}^*(\{\hat{Y}_{[1,M-1]}^e\}_{e \in \mathcal{E}}) G \end{aligned}$$

is an input-output trajectory of  $\Sigma$  readily follows from Theorem 2.(ii). If, in addition,  $L_0 \geq \ell_\Sigma$ , we have that

$$\ker \mathcal{O}_{L_0} = \ker \mathcal{O}_{L_0+m}, \text{ for all } m \in \mathbb{Z}_{\geq 1}. \quad (29)$$

Note that  $x_{-L_0}$  satisfying (26) may not be unique. In fact, the set of all  $x_{-L_0}$  satisfying (26) is given by

$$\begin{aligned} \mathbb{X}_{-L_0} &:= \xi + \ker \mathcal{O}_{L_0} \text{ with } \xi \in \mathbb{R}^{n_x} \text{ such that} \\ & y_{[-L_0, -1]} = \mathcal{O}_{L_0} \xi + \mathcal{T}_{L_0} u_{[-L_0, -1]}. \end{aligned}$$

Let  $\xi \in \mathbb{X}_{-L_0}$ . Then, the combined past and future output  $y_{[-L_0, L-1]}$  satisfy, for all  $\eta \in \ker \mathcal{O}_{L_0}$ ,

$$\begin{aligned} y_{[-L_0, L-1]} &= \mathcal{O}_{L_0+L}(\xi + \eta) + \mathcal{T}_{L_0+L} u_{[-L_0, L-1]} \stackrel{(29)}{=} \\ & \mathcal{O}_{L_0+L} \xi + \mathcal{T}_{L_0+L} u_{[-L_0, L-1]}. \end{aligned}$$

Thereby,  $y_{[0, L-1]}$  is unique.

#### D. Proof of Proposition 2

Let  $\{(\hat{U}_{[0, M-1]}^e, \hat{Y}_{[0, M-1]}^e)\}_{e \in \mathcal{E}}$  be a collection of input-output spectra of  $\Sigma$  satisfying Assumption 1. Suppose that  $\{\hat{U}_{[0, M-1]}^e\}_{e \in \mathcal{E}}$  is CPE of order  $L_0 + 1 + n_x$  with  $L_0 \in \mathbb{Z}_{\geq \ell_\Sigma}$ . Let  $z \in \mathbb{C}$  be a complex frequency that is not an eigenvalue of  $A$  and let  $U_z \in \mathbb{C}^{n_u}$  be the corresponding input spectrum.

For the (complex-valued) input sequence  $u_{[0, L_0]} = W_{L_0+1}(z) \otimes U_z$  and initial condition  $x_0 = (zI - A)^{-1} B U_z$ , we obtain, for all  $k \in \mathbb{Z}_{[0, L_0]}$ ,

$$\begin{aligned} y_k &= C A^k x_0 + C \sum_{j=0}^{k-1} A^{k-1-j} B u_j + D u_k = \quad (30) \\ & \left( C A^k (zI - A)^{-1} B + C \sum_{j=0}^{k-1} A^{k-1-j} B z^j + D z^k \right) U_z. \end{aligned}$$

If  $z = 0$ , then, since  $z$  is not an eigenvalue of  $A$ ,  $A$  must be invertible, and we obtain, for all  $k \in \mathbb{Z}_{[0, L_0]}$ ,

$$\begin{aligned} y_k &= \begin{cases} (C A^k (-A)^{-1} B + D) U_z, & \text{if } k = 0, \\ (C A^k (-A)^{-1} B + C A^{k-1} B) U_z, & \text{if } k \in \mathbb{Z}_{[1, L_0-1]}, \end{cases} \\ &= \begin{cases} (-C A^{k-1} B + D) U_z, & \text{if } k = 0, \\ 0, & \text{if } k \in \mathbb{Z}_{[1, L_0-1]}, \end{cases} \\ &= (C(zI - A)^{-1} B + D) z^k U_z = H(z) z^k U_z. \end{aligned}$$

If  $z \neq 0$ , we obtain, for all  $k \in \mathbb{Z}_{[0, L_0]}$ ,

$$\begin{aligned} y_k &= (C A^k (zI - A)^{-1} B + z^{k-1} C \sum_{j=0}^{k-1} (A z^{-1})^j B + D z^k) U_z, \\ &= (C A^k (zI - A)^{-1} B + \\ & \quad z^{k-1} C (I - (A z^{-1})^k) (I - A z^{-1})^{-1} B + D z^k) U_z, \\ &= (C A^k (zI - A)^{-1} B + \\ & \quad C (z^k I - A^k) (zI - A)^{-1} B + D z^k) U_z, \\ &= (C(zI - A)^{-1} B + D) z^k U_z = H(z) z^k U_z, \end{aligned}$$

where we used the fact that

$$\sum_{j=0}^{k-1} (A z^{-1})^j = (I - (A z^{-1})^k) (I - A z^{-1})^{-1}.$$

Let  $Y_z = H(z) U_z$ . It follows that both the real-valued pair of time-domain sequences  $(\Re(W_{L_0+1}(z) \otimes U_z), \Re(W_{L_0+1}(z) \otimes Y_z))$  and  $(\Im(W_{L_0+1}(z) \otimes U_z), \Im(W_{L_0+1}(z) \otimes Y_z))$  are input-output trajectories of  $\Sigma$  (with initial conditions  $x_0 = \Re((zI - A)^{-1} B U_z)$  and  $x_0 = \Im((zI - A)^{-1} B U_z)$ , respectively). By applying Theorem 2.(ii) (separately for  $(\Re(W_{L_0+1}(z) \otimes U_z), \Re(W_{L_0+1}(z) \otimes Y_z))$  and  $(\Im(W_{L_0+1}(z) \otimes U_z), \Im(W_{L_0+1}(z) \otimes Y_z))$ ) this is the case, if and only if there exist  $G_{0,r}, G_{0,i} \in \mathbb{R}^E$  and  $G_{1,r}, G_{1,i} \in \mathbb{C}^{E(M-1)}$  such that

$$\begin{aligned} \begin{bmatrix} W_{L_0+1}(z) \otimes U_z \\ W_{L_0+1}(z) \otimes Y_z \end{bmatrix} &= \\ \begin{bmatrix} \Re(W_{L_0+1}(z) \otimes U_z) + j \Im(W_{L_0+1}(z) \otimes U_z) \\ \Re(W_{L_0+1}(z) \otimes Y_z) + j \Im(W_{L_0+1}(z) \otimes Y_z) \end{bmatrix} &= \quad (31) \\ \begin{bmatrix} \mathcal{F}_{L_0+1}(\{\hat{U}_{[0, M-1]}^e\}_{e \in \mathcal{E}}) & \mathcal{F}_{L_0+1}^*(\{\hat{U}_{[1, M-1]}^e\}_{e \in \mathcal{E}}) \\ \mathcal{F}_{L_0+1}(\{Y_{[0, M-1]}^e\}_{e \in \mathcal{E}}) & \mathcal{F}_{L_0+1}^*(\{Y_{[1, M-1]}^e\}_{e \in \mathcal{E}}) \end{bmatrix} G, \end{aligned}$$

where

$$G = \begin{bmatrix} G_{0,r} + j G_{0,i} \\ \mathcal{G}_{1,r} + j \mathcal{G}_{1,i} \\ \mathcal{G}_{1,r}^* + j \mathcal{G}_{1,i}^* \end{bmatrix} = \underbrace{\begin{bmatrix} I & jI & 0 & 0 & 0 & 0 \\ 0 & 0 & I & jI & jI & -I \\ 0 & 0 & I & -jI & jI & I \end{bmatrix}}_{=: T_G \in \mathbb{C}^{E(2M-1) \times 2E(2M-1)}} \mathcal{G},$$

where  $\mathcal{G} = (G_{0,r}, G_{0,i}, \Re \mathcal{G}_{1,r}, \Im \mathcal{G}_{1,r}, \Re \mathcal{G}_{1,i}, \Im \mathcal{G}_{1,i})$ . Since  $\text{im } T_G = E(2M-1)$ , it follows that  $(W_{L_0+1}(z) \otimes U_z, W_{L_0}(z) \otimes Y_z)$  is a (complex-valued) input-output trajectory of  $\Sigma$  (with initial condition  $x_0 = (zI - A)^{-1} B U_z$ ), if and only if there exists  $G \in \mathbb{C}^{E(2M-1)}$  satisfying (31). Note that (31) is (10) rewritten.

We complete the proof by showing that  $Y_z$  is unique. To this end, note that, since  $L_0 \geq \ell_\Sigma$ , we have that (29) holds. We can, equivalently, write (30) as

$$W_{L_0}(z) \otimes Y_z = y_{[0, L_0-1]} = \mathcal{O}_{L_0} x_0 + \mathcal{T}_{L_0} (W_{L_0}(z) \otimes U_z). \quad (32)$$

Note that  $x_0$  satisfying (32) is not necessarily unique, however, it must belong to the set

$$\begin{aligned} \mathbb{X}_0 &:= \xi + \ker \mathcal{O}_{L_0} \text{ with } \xi \in \mathbb{C}^{n_x} \text{ such that} \\ & W_{L_0}(z) \otimes Y_z = \mathcal{O}_{L_0} \xi + \mathcal{T}_{L_0} (W_{L_0}(z) \otimes U_z). \end{aligned}$$

Let  $\xi \in \mathbb{X}_0$ . Then,  $y_{[0, L_0]} = W_{L_0+1}(z) \otimes Y_z$  satisfies

$$\begin{aligned} W_{L_0+1} \otimes Y_z &= \mathcal{O}_{L_0+1}(\xi + \eta) + \mathcal{T}_{L_0+1}(W_{L_0+1}(z) \otimes U_z) \\ &\stackrel{(29)}{=} \mathcal{O}_{L_0+1} \xi + \mathcal{T}_{L_0+1}(W_{L_0+1}(z) \otimes U_z), \end{aligned}$$

for all  $\eta \in \ker \mathcal{O}_{L_0}$ . Thus,  $y_{[0, L_0]}$  satisfying (30) is unique. It follows that  $W_{L_0+1}(z) \otimes Y_z$  in (31) and, thereby,  $Y_z$  (i.e., the first  $n_y$  entries of  $W_{L+1}(z) \otimes Y_z$ ) satisfying (10) are unique.

#### E. Proof of Proposition 3

Let  $(\hat{U}_{[0, M-1]}, \hat{Y}_{[0, M-1]})$  be an input-output spectrum of  $\Sigma$  in (1) satisfying Assumption 1. Suppose that  $\hat{U}_{[0, M-1]}$  is PE of order  $n_x + 1$  and that  $\text{rank} \begin{bmatrix} Q & \lambda I - A \end{bmatrix} = n_x$  for all  $\lambda \in \mathbb{C}$  with  $|\lambda| = 1$ . Then, by [44, Theorem 23], the optimal control law that achieves  $\lim_{k \rightarrow \infty} x_k = 0$  and minimizes the cost (12) is (11) with

$$\bar{K} = -(R + B^\top \bar{P} B)^{-1} B^\top \bar{P} A, \quad (33)$$

where  $\bar{P}$  is the *largest* real symmetric solution to the DARE

$$A^\top PA - P - A^\top PB(R + B^\top PB)^{-1}B^\top PA + Q = 0, \quad (34)$$

and satisfies  $\bar{P} \succcurlyeq 0$ . There is only one largest  $\bar{P}$  in the sense that any other solution  $\tilde{P}$  to (34) with  $\tilde{P} \succcurlyeq P$  for all  $P$  satisfying (34) must satisfy  $\tilde{P} = \bar{P}$  [44]. It follows that

$$(A + B\bar{K})^\top \bar{P}(A + B\bar{K}) - \bar{P} + \bar{K}^\top R\bar{K} + Q = 0. \quad (35)$$

Next, we show that  $\bar{P}$  is a solution to (14). To this end, let  $P = P^\top \in \mathbb{R}^{n_x \times n_x}$  be any symmetric matrix that satisfies  $\Delta^H \Psi(P) \Delta \succcurlyeq 0$ . Since  $X_1 = AX_0 + BU$ , it holds that

$$\Delta^H \Psi(P) \Delta = (\star)^H \begin{bmatrix} Q - P + A^\top PA & A^\top PB \\ B^\top PA & R + B^\top PB \end{bmatrix} \begin{bmatrix} X_0 \\ U \end{bmatrix}, \quad (36)$$

where, due to Theorem 2.(i), the matrix  $[X_0^\top \ U^\top]^\top$  has full row rank such that

$$\text{im} \begin{bmatrix} I \\ \bar{K} \end{bmatrix} \subset \text{im} \begin{bmatrix} X_0 \\ U \end{bmatrix} = \mathbb{C}^{n_u + n_x}.$$

Since  $\Delta^H \Psi(P) \Delta \succcurlyeq 0$ , it follows that

$$0 \preceq (\star)^\top \begin{bmatrix} Q - P + A^\top PA & A^\top PB \\ B^\top PA & R + B^\top PB \end{bmatrix} \begin{bmatrix} I \\ \bar{K} \end{bmatrix} = (A + B\bar{K})^\top P(A + B\bar{K}) - P + \bar{K}^\top R\bar{K} + Q.$$

Subtracting (35) from this yields

$$(\bar{P} - P) - (A + B\bar{K})^\top (\bar{P} - P)(A + B\bar{K}) \succcurlyeq 0,$$

which, since  $A + B\bar{K}$  is Schur, implies that  $\bar{P} \succcurlyeq P$ . We conclude that  $\bar{P} \succcurlyeq P$  for any  $P$  that satisfies  $\Delta^H \Psi(P) \Delta \succcurlyeq 0$ . It follows that  $\text{tr} \bar{P} \geq \text{tr} P$ . In addition,  $\bar{P}$  satisfies

$$\Delta^H \Psi(\bar{P}) \Delta = 0 \succcurlyeq 0.$$

Hence, we can conclude that  $\bar{P}$  is a solution to (14).

To show that  $\bar{P}$  is the unique solution to (14), let  $\tilde{P}$  be another solution to (14). Then,  $\tilde{P} = \tilde{P}^\top \succcurlyeq 0$ ,  $\text{tr} \tilde{P} = \text{tr} \bar{P}$ , and  $\Delta^H \Psi(\tilde{P}) \Delta \succcurlyeq 0$ . It follows, as we have shown above, that  $\tilde{P} \succcurlyeq \bar{P}$ . Thereby, all eigenvalues of  $\tilde{P} - \bar{P}$ , denoted  $\{\lambda_i(\tilde{P} - \bar{P})\}_{i=1}^{n_x}$ , are non-negative, i.e.,  $\tilde{P} - \bar{P} \succcurlyeq 0$ . In addition, we know that  $0 = \text{tr} \tilde{P} - \bar{P} = \sum_{i=1}^{n_x} \lambda_i(\tilde{P} - \bar{P})$ , which, combined with  $\tilde{P} - \bar{P} \succcurlyeq 0$ , implies that all eigenvalues of  $\tilde{P} - \bar{P}$  are zero. Since  $\tilde{P} - \bar{P}$  is symmetric, it follows from the eigenvalue decomposition that  $\tilde{P} - \bar{P} = 0$ , and, hence,  $\tilde{P}$  is the unique solution to (14).

It remains to show that  $\bar{K}$ , i.e., the optimal control law (11) that minimizes (12) and achieves  $\lim_{k \rightarrow \infty} x_k = 0$ , can be computed as (13). To this end, observe that we can express

$$\begin{aligned} \Delta^H \Psi(\bar{P}) \Delta &\stackrel{(36)}{=} (\star)^H \begin{bmatrix} A^\top \bar{P}A - \bar{P} + Q & A^\top \bar{P}B \\ B^\top \bar{P}A & R + B^\top \bar{P}B \end{bmatrix} \begin{bmatrix} X_0 \\ U \end{bmatrix} \\ &\stackrel{(34)}{=} (\star)^H \begin{bmatrix} (R + B^\top \bar{P}B)^{-1} & I \\ I & R + B^\top \bar{P}B \end{bmatrix} \begin{bmatrix} B^\top \bar{P}AX_0 \\ U \end{bmatrix} \\ &= (\star)^H \begin{bmatrix} R + B^\top \bar{P}B & -(R + B^\top \bar{P}B) \\ -(R + B^\top \bar{P}B) & R + B^\top \bar{P}B \end{bmatrix} \begin{bmatrix} \bar{K}X_0 \\ U \end{bmatrix} \\ &= (U - \bar{K}X_0)^H (R + B^\top \bar{P}B)(U - \bar{K}X_0), \end{aligned} \quad (37)$$

where  $\bar{K}$  is the optimal feedback gain in (33). Due to Theorem 2.(i), there exists  $\Gamma \in \mathbb{C}^{2M-1 \times n_x}$  such that

$$\begin{bmatrix} X_0 \\ U \end{bmatrix} \Gamma = \begin{bmatrix} I \\ \bar{K} \end{bmatrix}.$$

Note that this implies that  $\Gamma$  is a right inverse of  $X_0$ , whereby  $\Gamma X_0 \Gamma = \Gamma$  and, since  $\Delta^H \Psi(\bar{P}) \Delta = 0$ , it follows that

$$\Delta^H \Psi(\bar{P}) \Delta \Gamma = (U - \bar{K}X_0)^H (R + B^\top \bar{P}B)(U \Gamma - U \Gamma X_0 \Gamma) = 0.$$

This shows that there exists a right inverse  $X_0^\dagger$  of  $X_0$  such that  $\Delta^H \Psi(\bar{P}) \Delta X_0^\dagger = 0$ . If  $X_0^\dagger$  is a right inverse of  $X_0$  satisfying  $\Delta^H \Psi(\bar{P}) \Delta X_0^\dagger = 0$ , then it follows from (37), due to  $R + B^\top \bar{P}B \succ 0$ , that  $(U - \bar{K}X_0)X_0^\dagger = 0$ . We conclude that the optimal feedback gain satisfies  $K = \bar{K} = UX_0^\dagger$ .

## F. Proof of Theorem 3

Let  $\{(\hat{U}_{[0, M-1]}^e, \hat{Y}_{[0, M-1]}^e)\}_{e \in \mathcal{E}}$  and  $(\hat{u}_{[0, N-1]}, \hat{y}_{[0, N-1]})$  be, respectively, a collection of input-output spectra and a trajectory of  $\Sigma$  in (1) satisfying Assumption 1. Suppose that  $\{\hat{U}_{[0, M-1]}^e\}_{e \in \mathcal{E}}$  and  $\hat{u}_{[0, M-1]}$  are, respectively, CPE and PE of order  $\bar{T} + T + n_x$ . Observe that, if  $\lambda_g = \lambda_G = 0$ , the only difference between (16) and (3) is in the precise matrix-vector product used in the prediction model to express the input-output trajectory

$$\left( \begin{bmatrix} u_{[k-\bar{T}, k-1]} \\ u_{[0, T-1], k} \end{bmatrix}, \begin{bmatrix} y_{[k-\bar{T}, k-1]} + \sigma_k \\ y_{[0, T-1], k} \end{bmatrix} \right).$$

Hence, to show that (16) and (3) admit the same (set of) optimal control action(s), it suffices to show that

$$\begin{aligned} \text{im} \left[ \frac{H_{\bar{T}+T}(\hat{u}_{[0, N-1]})}{H_{\bar{T}+T}(\hat{y}_{[0, N-1]})} \right] &= \\ \text{im} \left[ \frac{\mathcal{F}_{\bar{T}+T}(\{\hat{U}_{[0, M-1]}^e\}_{e \in \mathcal{E}})}{\mathcal{F}_{\bar{T}+T}(\{\hat{Y}_{[0, M-1]}^e\}_{e \in \mathcal{E}})} \frac{\mathcal{F}_{\bar{T}+T}^*(\{\hat{U}_{[1, M-1]}^e\}_{e \in \mathcal{E}})}{\mathcal{F}_{\bar{T}+T}^*(\{\hat{Y}_{[1, M-1]}^e\}_{e \in \mathcal{E}})} \right], \end{aligned}$$

which follows by combining Lemma 1.(ii) and Theorem 2.(ii).

## REFERENCES

## REFERENCES

- [1] J. Berberich and F. Allgöwer, "A trajectory-based framework for data-driven system analysis and control," in *Eur. Control Conf.*, 2020, pp. 1365–1370.
- [2] C. Verhoek, R. Tóth, S. Haesaert, and A. Koch, "Fundamental lemma for data-driven analysis of linear parameter-varying systems," in *60th IEEE Conf. Decis. Control*, 2021, pp. 5040–5046.
- [3] J. C. Willems, P. Rapisarda, I. Markovsky, and B. L. M. De Moor, "A note on persistency of excitation," *Syst. Control Lett.*, vol. 54, no. 4, pp. 325–329, 2005.
- [4] H. J. van Waarde, C. De Persis, M. K. Camlibel, and P. Tesi, "Willems' fundamental lemma for state-space systems and its extension to multiple datasets," *IEEE Control Syst. Lett.*, vol. 4, no. 3, pp. 602–607, 2020.
- [5] M. Verhaegen and P. Dewilde, "Subspace model identification Part 1. The output-error state-space model identification class of algorithms," *Int. J. Control*, vol. 56, no. 5, pp. 1187–1210, 1992.
- [6] O. Molodchyk and T. Faulwasser, "Exploring the links between the fundamental lemma and kernel regression," *IEEE Control Syst. Lett.*, vol. 8, pp. 2045–2050, 2024.
- [7] P. Schmitz, T. Faulwasser, and K. Worthmann, "Willems' fundamental lemma for linear descriptor systems and its use for data-driven output-feedback MPC," *IEEE Control Syst. Lett.*, vol. 6, pp. 2443–2448, 2022.

- [8] T. Faulwasser, R. Ou, G. Pan, P. Schmitz, and K. Worthmann, “Behavioral theory for stochastic systems? A data-driven journey from Willems to Wiener and back again,” *Annu. Rev. Control*, vol. 55, pp. 92–117, 2023.
- [9] G. Pan, R. Ou, and T. Faulwasser, “On a stochastic fundamental lemma and its use for data-driven optimal control,” *IEEE Trans. Autom. Control*, 2022.
- [10] R. Rapisarda, M. K. Çamlıbel, and H. J. van Waarde, “A ‘fundamental lemma’ for continuous-time systems, with applications to data-driven simulation,” *Syst. Control Lett.*, vol. 179, p. 105603, 2023.
- [11] J. Coulson, J. Lygeros, and F. Dörfler, “Data-enabled predictive control: In the shallows of the DeePC,” in *Eur. Control Conf.*, 2019, pp. 307–312.
- [12] P. C. N. Verheijen, V. Breschi, and M. Lazar, “Handbook of linear data-driven predictive control: Theory, implementation and design,” *Annu. Rev. Control*, vol. 56, p. 100914, 2023.
- [13] C. Verhoek, H. S. Abbas, R. Tóth, and S. Haesaert, “Data-driven predictive control for linear parameter-varying systems,” *IFAC-PapersOnLine*, vol. 54, no. 8, pp. 101–108, 2021.
- [14] D. Bilgic, A. Harding, and T. Faulwasser, “Data-driven predictive control of bilinear HVAC dynamics—An experimental case study,” *IEEE Control Syst. Lett.*, vol. 8, pp. 3009–3014, 2024.
- [15] J. Berberich, J. Köhler, M. A. Müller, and F. Allgöwer, “Linear tracking MPC for nonlinear systems—Part II: The data-driven case,” *IEEE Trans. Autom. Control*, vol. 67, no. 9, pp. 4406–4421, 2022.
- [16] M. Alsati, V. G. Lopez, J. Berberich, F. Allgöwer, and M. A. Müller, “Data-driven nonlinear predictive control for feedback linearizable systems,” *IFAC-PapersOnLine*, vol. 56, no. 2, pp. 617–624, 2023.
- [17] M. Lazar, “Basis functions nonlinear data-enabled predictive control: Consistent and computationally efficient formulations,” 2023, preprint: <https://arxiv.org/abs/2311.05360>.
- [18] A. Azarbahram, M. Al Khatib, V. K. Mishra, and N. Bajcinca, “Data-driven predictive control for a class of nonlinear systems with polynomial terms,” *IFAC-PapersOnLine*, vol. 58, no. 21, pp. 226–231, 2024.
- [19] G. Pan, R. Ou, and T. Faulwasser, “Towards data-driven stochastic predictive control,” *Int. J. Robust Nonlinear Control*, pp. 1–23, 2023.
- [20] V. Breschi, A. Chiuso, and S. Formentin, “Data-driven predictive control in a stochastic setting: A unified framework,” *Automatica*, vol. 152, p. 110961, 2023.
- [21] G. F. Franklin, J. D. Powell, and A. Emami-Naeini, *Feedback control of dynamic systems*, 6th ed. Pearson, 2010.
- [22] S. Skogestad and I. Postlethwaite, *Multivariable feedback control: Analysis and design*, 2nd ed. Wiley, 2005.
- [23] R. Pintelon and J. Schoukens, *System Identification: A Frequency Domain Approach*. Wiley, 2012.
- [24] E. Evers, “Identification and active thermomechanical control in precision mechatronics,” Ph.D. dissertation, Technische Universiteit Eindhoven, 2021.
- [25] T. Söderström and P. Stoica, *System identification*. Prentice Hall, 1989.
- [26] M. Ferizbegovic, H. Hjalmarsson, P. Mattsson, and T. B. Schön, “Willems’ fundamental lemma based on second-order moments,” in *60th IEEE Conf. Decis. Control*, 2021, pp. 396–401.
- [27] I. Markovsky and H. Ossareh, “Finite-data nonparametric frequency response evaluation without leakage,” *Automatica*, vol. 159, p. 111351, 2024.
- [28] L. Özkan, J. Meijjs, and A. C. P. M. Backx, “A frequency domain approach for MPC tuning,” *Comput. Aided Chem. Eng.*, vol. 31, pp. 1632–1636, 2012.
- [29] J. G. Burgos, C. A. López Martínez, R. van de Molengraft, and M. Steinbuch, “Frequency domain tuning method for unconstrained linear output feedback model predictive control,” in *Proc. 19th IFAC World Congress*, 2014, pp. 7455–7460.
- [30] G. Shah and S. Engell, “Multivariable MPC design based on a frequency response approximation approach,” in *Eur. Control Conf.*, 2013, pp. 13–18.
- [31] K. K. Sathyanarayanan, G. Pan, and T. Faulwasser, “Towards data-driven predictive control using wavelets,” *IFAC-PapersOnLine*, vol. 56, no. 2, pp. 632–637, 2023.
- [32] T. J. Meijer, S. A. N. Nouwens, K. J. A. Scheres, V. S. Dolk, and W. P. M. H. Heemels, “Frequency-domain data-driven predictive control,” *IFAC-PapersOnLine*, vol. 58, no. 18, pp. 86–91, 2024.
- [33] C. De Persis and P. Tesi, “Formulas for data-driven control: Stabilization, optimality, and robustness,” *IEEE Trans. Autom. Control*, vol. 65, no. 3, pp. 909–924, 2020.
- [34] —, “Low-complexity learning of linear quadratic regulators from noisy data,” *Automatica*, vol. 128, p. 109548, 2021.
- [35] I. Markovsky, J. C. Willems, P. Rapisarda, and B. L. M. De Moor, “Algorithms for deterministic balanced subspace identification,” *Automatica*, vol. 41, pp. 755–766, 2005.
- [36] I. Markovsky, J. C. Willems, S. Van Huffel, and B. De Moor, *Exact and approximate modeling of linear systems: A behavioral approach*. SIAM, 2006.
- [37] J. Berberich, J. Köhler, M. A. Müller, and F. Allgöwer, “Data-driven model predictive control with stability and robustness guarantees,” *IEEE Trans. Autom. Control*, vol. 66, no. 4, 2021.
- [38] T. McKelvey, H. Akcay, and L. Ljung, “Subspace-based multivariable system identification for frequency response data,” *IEEE Trans. Autom. Control*, vol. 41, no. 7, pp. 960–979, 1996.
- [39] P. Van Overschee and B. De Moor, “Continuous-time frequency domain subspace system identification,” *Signal Process.*, vol. 52, pp. 179–194, 1996.
- [40] B. Caubergh, P. Guillaume, R. Pintelon, and P. Verboven, “Frequency-domain subspace identification using frf data from arbitrary signals,” *J. Sound Vib.*, vol. 290, pp. 555–571, 2006.
- [41] T. J. Meijer, S. A. N. Nouwens, V. S. Dolk, and W. P. M. H. Heemels, “A frequency-domain version of Willems’ fundamental lemma,” 2023, preprint: <https://arxiv.org/abs/2311.15284>.
- [42] J. G. Proakis and D. G. Manolakis, *Digital Signal Processing: Principles, Algorithms and Applications*. Prentice Hall, 1996.
- [43] G. C. Walsh and H. Ye, “Scheduling of networked control systems,” *IEEE Control Syst. Mag.*, vol. 21, no. 1, pp. 57–65, 2001.
- [44] H. J. van Waarde, J. Eising, H. L. Trentelmann, and M. K. Camlibel, “Data informativity: A new perspective on data-driven analysis and control,” *IEEE Trans. Autom. Control*, vol. 65, no. 11, pp. 4753–4768, 2020.
- [45] M. van Berkel, “Estimation of heat transport coefficients in fusion plasmas,” Ph.D. dissertation, Technische Universiteit Eindhoven, 2015.